1991

Modeling of CBN wheels and creep-feed grinding process for off- line multi-objective optimization

I-Chung Joseph Lin
Lehigh University

Modeling of CBN Wheels and Creep-Feed Grinding Process for Off-Line Multi-Objective Optimization

by

I-Chung Joseph Lin

A Thesis
Presented to the Graduate Committee
of Lehigh University
in Candidacy for the Degree of
Master of Science
in
Industrial Engineering

Lehigh University
1991

This thesis is accepted and approved in partial fulfillment of the requirements for the degree of Master of Science in Industrial Engineering

5/13/91

Date

Dr. G. Sathyanarayanan

Professor in Charge

Dr. John W. Adams

Acting Chairman, Industrial Eng. Dept.

Acknowledgments

I would like to thank Dr. Sathyanarayanan for his time, help and encouragement all through my association with him. I would like to thank Dr. Adams for the help he offered me as a teacher and friend.

Mr. M. K. Chen, Mr. J.C. Fu and Miss Xi Gao deserved special mention among numerous friends who have contributed to this research.

I would like to express my sincere gratitude to my family members for their endless support.

Table of Contents

Abstract

Creep-feed grinding of superalloys is modeled and analyzed in this thesis. For the experimental data, a dedicated neural network was trained with few iterations to provide an intelligent system which integrated multiple sensors.

The trained neural network was utilized to optimize the grinding process. An off-line optimization procedure was carried out by utilizing a Multiple Criteria Decision Making (MCDM) technique. Several conflicts among the system outputs were satisfied to achieve the overall optimality. Many alternate solutions were also given to suggest a process strategy for the given constraints of the problem.

Grinding wheel profile was digitized to achieve a model. Several possible approaches to simulate the topography were identified. Fractal modeling turned out to be the most useful methodology. Fractal properties of the wheel surface has been explored. With fractal analysis, the wheel surface topography was successfully characterized and regenerated by simulation with remarkable accuracy.

Dynamic active cutting edges in the cutting zone for certain working conditions have been obtained. Binary codes associated with each edge constitute to zero-one series which was then used to accomplish a four-state markov chain problem formulation. A C++ object oriented module was implemented to fulfill the necessary task.

Chapter1
Introduction

1.1 Research Problem

As more and more materials are introduced, the machining techniques have become a major concern for manufacturing industry. The techniques emphasize not only on the efficiency of the production process but also the product accuracy that can be achieved with the process.

Grinding process is used as a finishing operation. In terms of machining aerospace alloys, conventional Al_2O_3 abrasive wheels is not in favor due to the high wheel wear rate in creep feed mode. Creep feed grinding with CBN or diamond abrasive wheels is suitable to meet the requirement of productivity and accuracy. Extensive utilization of CBN or diamond wheels will provide desirable properties like:

1. High hardness - provides greater ability to scratch or indent another material [1].
2. High thermal conductivity - a large portion of the heat is dissipated through the wheel thus preventing thermal damage to the work materials. [1-3]
3. Produces residual compressive stress[3-6].
4. Low wear rate - long wheel life [7].

Though diamond and CBN wheels both possess the above properties, the chemical instability of diamond in the presence of iron has made CBN wheels the only alternative to machine hard to machine alloy steels.

The optimal performance of grinding process can be ensured by a careful and systematic selection of working conditions. But due to the complexity of the process, making such a judgement is not an easy task. Besides, the existence of a conflict between objectives makes the problem even more complex. For example, a maximum material removal rate can be achieved by increasing feed rate and depth of cut, but this causes a negative effect on the surface finish. Traditionally, economical criteria such as cost, production or profit rate are utilized to achieve optimal machining operations. However, this rule is too general to be applied to a specific process. It is necessary for the current research to develope a dedicated optimization methodology that relates inputs such as feed rate, depth of cut and the other factors to outputs like power, force and surface finish. A simultaneous satisfaction of all the objectives is then accomplished by adjusting the parameters in the methodology.

The optimization procedure relies on an accurate description of the system behavior. That is to say, an underlying model has to be developed to help in the selection of working conditions. For the purpose of the system integration, the model must accurately describe the system and provide concurrent processing and sensing ability to serve as an on-line controller. Adaptability of the embedded model is required once the system behavior is changed due to the variation in the environment.

In order to explore the grinding mechanism completely, it is necessary to investigate the micro event that occurs during the process. The grinding system behavior is due to the interactions between work material and every single grit present in the cutting zone. Due to this interaction, the grinding

process produces wear which is represented as a feed back system in *Figure 1.1.*

As shown in *Figure 1.1*, the kinematic aspects associated with the grinding process can be represented. The abrasive-material engagement is dominated by the irregular distribution of the wheel geometry. As a result of this engagement, chips are formed and removed, outputs such as force, heat and surface finish are generated. Fracture and plastic deformation produced during the engagement constitute to the modification of both work piece and abrasive grains topography. And this completes the loop as shown in *Figure 1.1.*

It is thus obvious that the wheel topography is one of the most predominant factor that affects the overall performance. An accurate description of the wheel profile is very desirable. This is difficult to achieve because the wheel surface is as small as micro meter. The stylus is often used to characterize the wheel surface. The profilometer records the data by magnifying the magnitude of the movement of the stylus when it traverses across the wheel. As soon as the data is collected, analysis should be carried out to recognize and then simulate the surface to a desirable degree.

A methodology that can capture most of the quantitative and qualitative information from the wheel topographic data is developed in this thesis.

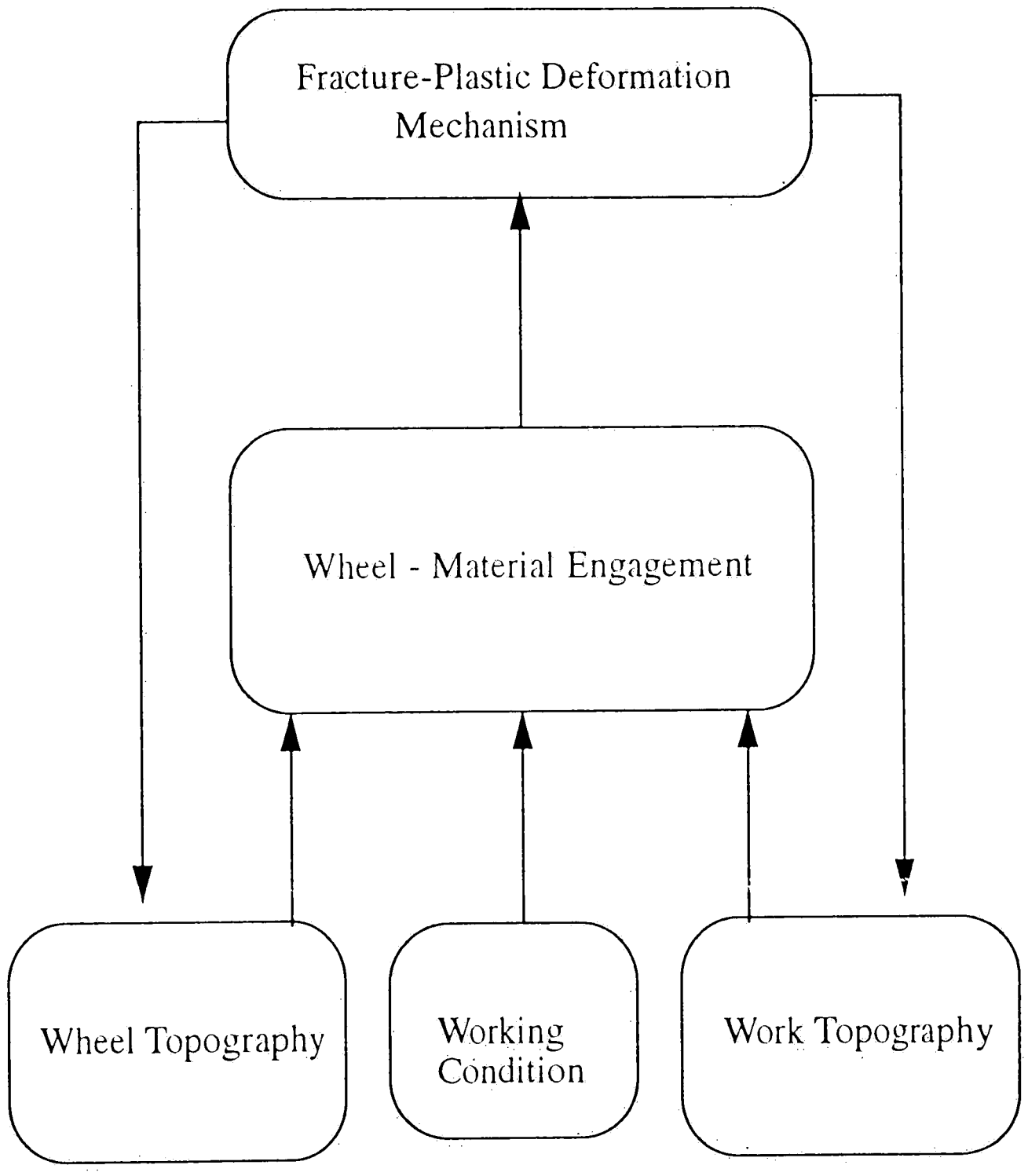

Figure 1.1 A Feed Back System of Grinding Process

1.2 Research Objective

The current research focuses on:

1. Neural Network Modeling:

   Develop an intelligent integrated sensor model which concurrently monitors several system inputs (bond type, feed rate and depth of cut) and provide models for multi-objectives optimization of the grinding process.

2. Multiple Objective Optimization

   Mathematical formulation of the grinding process as a multi-objective optimization problem. The solution set for the multi-objective problem should provide a process strategy that explicitly specifies the optimal working parameters for the grinding process.

3. Modeling and Analysis of Grinding Wheel topography.

   Provide an accurate topographical description for the wheel surtace. Based on the experimental data, formulate a simulation for the wheel profile which will, in turn, serve as an input for further analysis.

4. Calculation and stochastic analysis of active cutting edges by applying Markov chain theory.

The procedure for the present research is represented as a flow diagram and shown in *Figure 1.2.* and *Figure 1.3.*

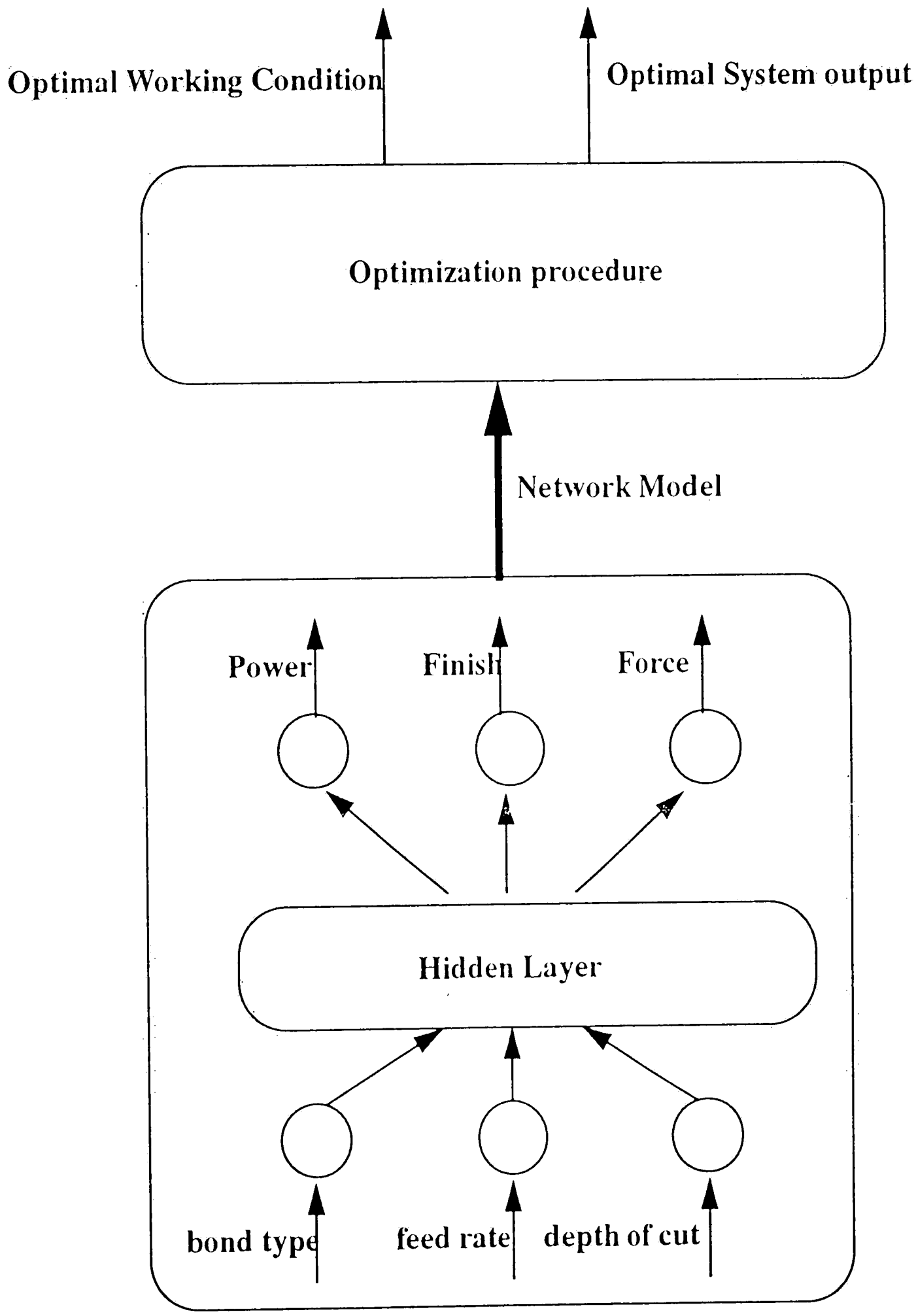

Figure 1.2. Neural Network Modeling of Grinding Process

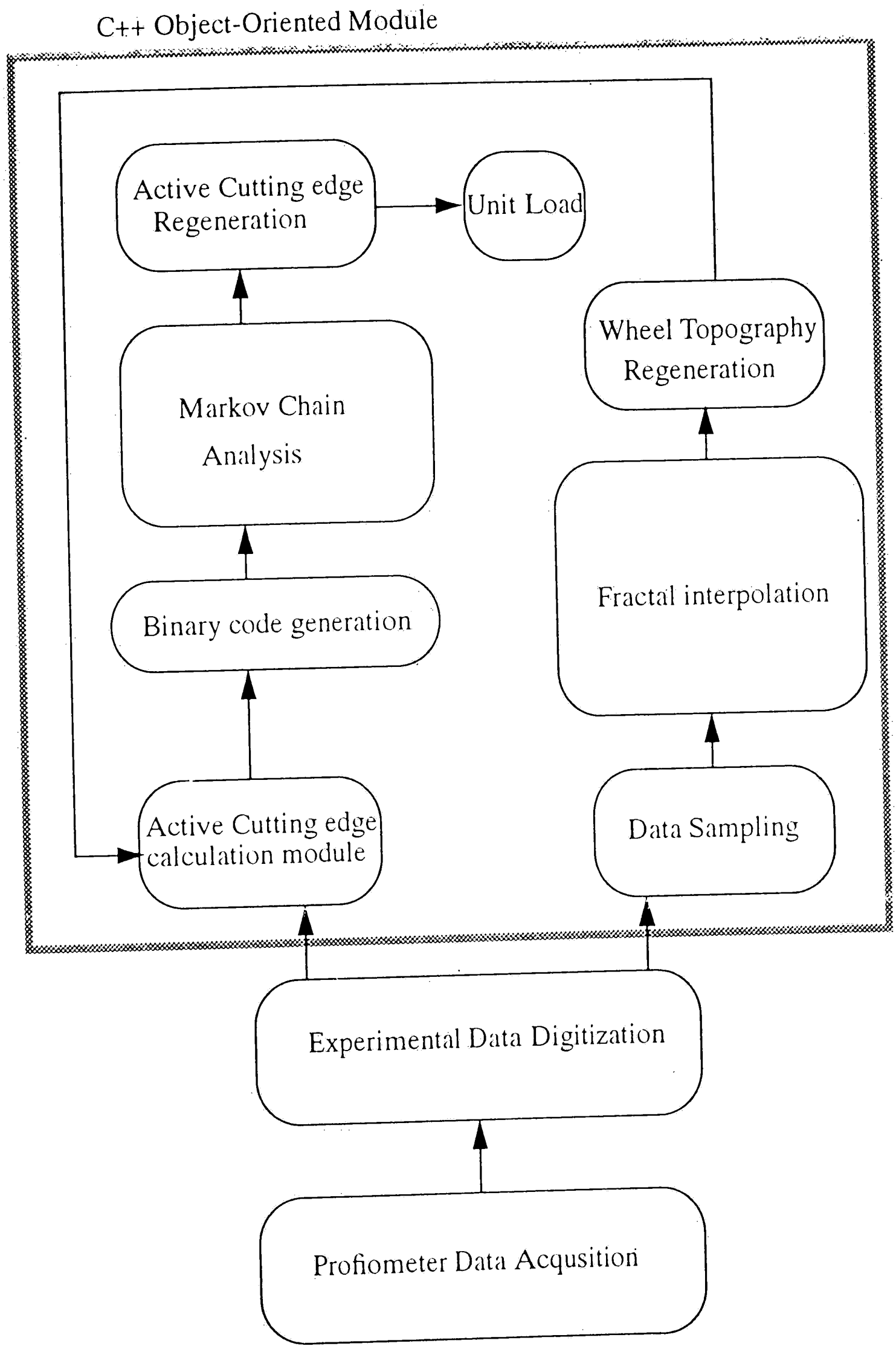

Figure 1.3. Object Oriented Module of Surface Analysis

Chapter 2

Literature Review

2.1 Grinding Process

Grinding is a material removal process which is carried out by a rotating abrasive wheel. Material is removed by a shearing process. Grinding is similar to milling operation because of many irregular grains randomly distributed on the wheel circumference. According to Kalpakjian[8], there are four different types of grinding operations, namely, surface, cylindrical, internal and centerless grinding.

A typical grinding system involves identifying the appropriate input and output parameters of the system. The inputs include parameters such as feed rate, depth of cut, wheel property and work material specification. The outputs can be analyzed with grinding power, grinding force and surface finish and component accuracy. Such a system is shown in *Figure 2.1*.

2.1.1 Introduction

In this section, creep feed grinding is first discussed. The comparison of performance between creep feed and conventional grinding is reviewed. Section 2.1.2 is concerned with the modeling technique that is used for the grinding process. Regression and slip-line techniques are also discussed.

The modeling of the wheel topography is reviewed in section 2.1.3. In this section, methodologies about surface measurement and surface regeneration by fractal methodology are reviewed. The last section discusses the issue per-

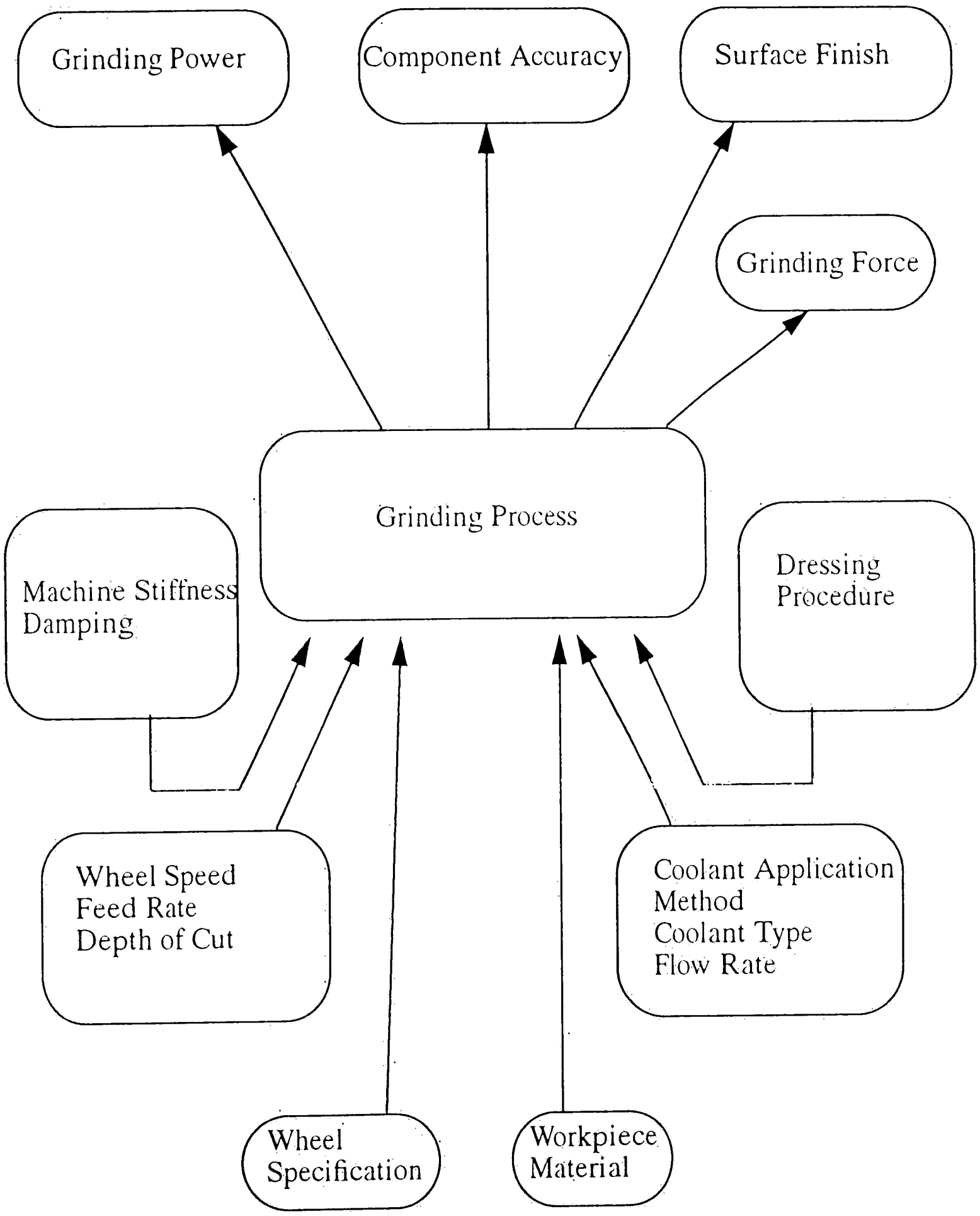

Figure.2.1 Grinding Process Input/Output Relation Diagram

taining to wheel characterization. Possible approaches like time series and stochastic simulation are also included in this section.

2.1.2 Creep Feed Grinding

Creep feed grinding is basically a stock removal process, although, depending on the requirement, it can produce components without any need for further finishing operation. Creep-feed grinding is operated with a low feed rate (10-1000 mm/min) and high depth of cut (1-10mm or larger) versus the high feed rate (5-25 m/min) and low depth of cut (2-25μm) required in conventional grinding [9]. Therefore, the material remove rate from creep feed grinding is about twenty times that of the conventional grinding.

As shown in [10], three types of creep grinding are used in the U.S. industry today, namely, pseudo creep feed, true creep feed and continuous dressing creep feed. The configurations for each type of creep feed grinding are presented in *Figure 2.2*

The performance of creep feed and pendulum grinding are compared in the following paragraphs. Werner [10] has developed an expression for the normal grinding force which suggests that creep feed grinding require higher force and specific energy than pendulum grinding for grinding materials classified as "difficult-to-grind". Measurements of profile wear on the wheel corner have been carried out on V-shaped profiles [9]. The finding indicates that the wear is less for the creep-feed grinding conditions. In [11], a formula for the surface finish produced by both creep feed and pendulum grinding has been proposed. The formula shows that in creep feed grinding, surface finish can be improved by increasing the wheel speed.

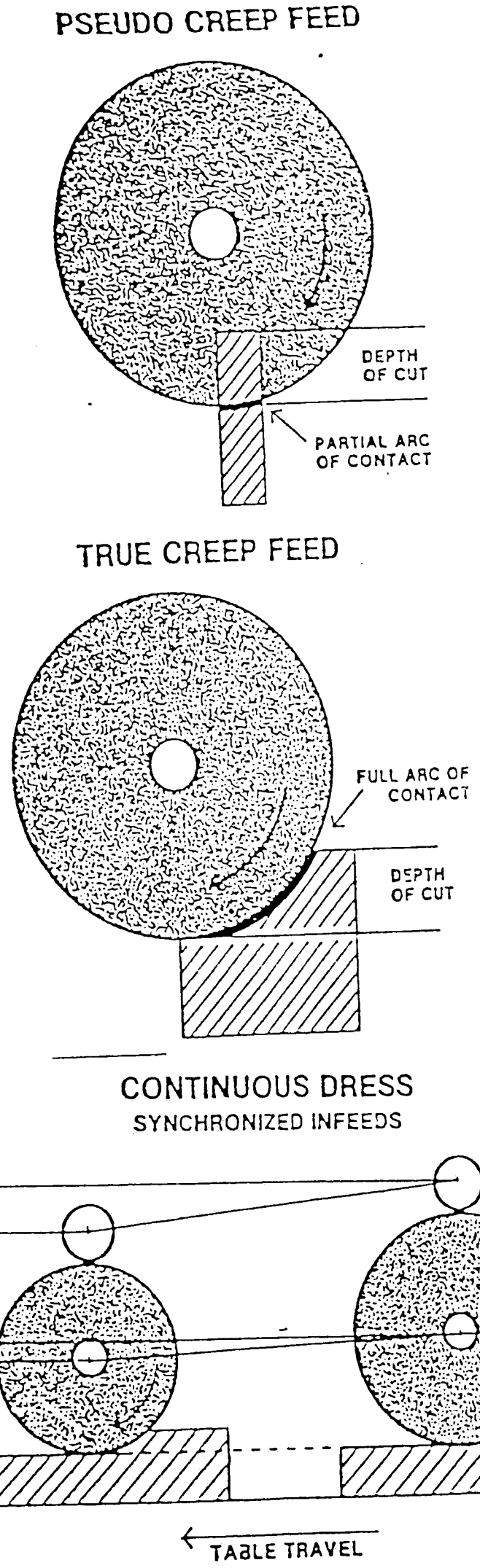

Figure 2.2 Three Types of Creep Feed Grinding

2.1.3 Modeling the Grinding Process

A great deal of effort has been spent in modeling the grinding mechanism. Rubenstein[12] has derived a linear relation between the normal and tangential force based on the assumptions for the wheel - workpiece contact, grit category, normal and tangential forces equation, hardness pressure of the workpiece and the ploughing pressure of the workpiece. The useful wheel life was also predicted in this paper that corresponds, largely, with the period during which the plateau area per grit increases. During this period, the grit wear is found to be dominated exclusively by attritious wear.

In [13], the stages from friction to ploughing and cutting has been described by utilizing a slip-line field which satisfies all the existing boundary conditions by starting from the velocity relation at the average penetrating cutting edge and characterizing the frictional condition at the interface between the cutting edge and the work material. On the basis of this model, it has been shown that there exists a critical depth of cut before a chip formation arises leading to material removal.

Wetton[14] has compared the theoretical production of a frontal bulge and lateral walls by modifying the slip-line field in the presence of friction. The theory explains the transition from the formation of a frontal bulge to continuous swarf or to continuous chips. It is suggested that this approach could be extended to a general sliding problem in which the formation of a frontal bulge, wedge or prow is observed.

An empirical model for creep-feed grinding [15] has been derived by utilizing a factorial experimental design. The model simplified each input term

by truncating higher order effects. Trends for surface finish, force and specific energy versus every input are obtained in this report.

2.1.4. Wheel Surface Modeling of Wheel Topography

The behavior of the grinding process can be further explored by an appropriate modeling of the wheel topography. Several works on the topographical model have been carried out.Shah and Malkin[16], have developed an on-line computer-controlled profilometer which was utilized for quantitative characterization of extremely rough surfaces like grinding wheels and coated abrasives. In the developed system, the stylus oscillated while the surface below moved incrementally so that the surface was stationary when contacted by the stylus.

In [17], the Electrical Discharge (ED) machined surface were studied by using Scanning Electron Microscopy (SEM) and profilometer. Relations between EDM conditions, workpiece material, microscopic analysis and fractal and conventional analysis of profiles, were found. It was concluded that it is suitable to associate noticeable features of the micrographs with parameters derived from rectal and conventional analysis of Profilometer data. The fractal analysis resulted in parameters (fractal dimension) which appeared to contain different information about the profile than the conventional parameters.

Nayak [18] has modeled rough surfaces as a two-dimensional, isotropic, Gaussion random process with the help of random process theory analysis. It was found that all higher order surface statistics depended only on the param-

eters obtained from a single profile for Gaussion isotropic surfaces, and from three nonparallel profiles for Gaussion and nonisotropic surfaces.

By employing parametric stochastic models of autoregressive-moving average (ARMA), DeVor and Wu [19] have implemented a technique for surface profile characterization. The analysis was established through the criteria of ergodicity, sensitivity and describability. With 95 percent confidence level, models for profile generated and recorded under identical conditions were statistically equivalent. At 95 percent confidence interval, the models were found to detect differences in the structure of the profile generated under identical machining conditions but was different at different location along the progression of the cut. The descriptive ability of the ARMA models was shown by relating the individual model parameters to the various physical components of the surface texture.

Fractal analysis is another approach used in modeling the surface geometry. Variety of theories and applications have been developed for fractal geometry[20-24]. In [25], fractal landscape with dimensions between two and three were generated by layering Brownian surfaces.

2.1.5. Grinding Wheel Surface Characterization

In order to obtain a meaningful information from either simulated or experimental data, one will be concerned with the characterization of the data. The micro structure and the detailed analysis of the mechanism can be achieved by the effective transformation or characterization of the data.

In [26], a new apparatus was developed to visually present the behavior of abrasive grits during the grinding process. A method for calculating the effective grain spacing to determine the distribution of cutting edges, as well as the cutting edge ratio for known worn grain conditions has been derived. Conclusions are:

1. Construction and distribution of cutting edges are largely affected by the dressing methods and conditions.

2. When making the first grinding pass, the top of the grains wear, and the worn surface is thrown up so that the working surface of the wheel comes into contact with worn grains.

3. The worn grain surfaces have many scratches very similar to those of finished metal surfaces.

An exploratory attempt has been made to study the grinding process with respect to the surface topography and nature of surface interaction by simulation[27]. The simulated results indicate the potentiality of the simulation method in analyzing the grinding process. Percentage of active cutting grains and effective grain spacings were also obtained by simulation. Poorer surface finish was predicted for grinding with high feed rate, higher wheel speed and coarsely dressed wheel.

McAdams[28] analyzed the abrasive profile by means of Markov chain theory. The Chapman-Kolmogrov equations were utilized to investigate the distances between successive cutting edges and the lengths of lands on a worn grinding surface. A first order- two states Markov chain was formulat-

ed. The state space consists of grits protruding above a reference line being coded as 1 and the rest of the grits were coded as 0.

Malkin [29] has presented a mathematical analysis of the cutting geometry during grinding, arising from consideration of the kinematic interactions between the topography of the grits and workpiece. Aside from leading to fundamental parameters, such as undeformed chip thickness, the size of the grinding zone and the contact length, a basis for analyzing the abrasive interactions with workpiece, the grinding temperature and the geometry of the ground surface generated have been constructed.

2.2 Neural Network

The conventional approach to the modeling of the grinding process, as discussed in the previous paragraph, suffers from few limitations. First, a large amount of empirical data has to be generated in order to model the system response accurately in the traditional way. Secondly, due to the conventional serial computing process, the derived model can't adjust itself for simultaneous changes in the parameters. Hence, a new modeling technique by Artificial Neural Network(ANN) for the grinding process as will be discussed in the following sections is proposed. The ANN is shown in the following sections can overcome the limitation of the previous modeling techniques.

2.2.1 Introduction

Neural networks are so named since their design is derived from the neural structure of the human brain. There are two types of neural network: Biological neural networks and artificial neural networks (ANN) [30]. The human brain is a biological neural network. The basic element of the human brain is the basic cell called the "neuron". A neuron consists of four elementary components: dendrites, soma, axon, and synapses. The dendrites are the input channels and are the extensions of the soma. Through the synapses, the dendrites receive the excitation or inhibition signal from other cells. The soma is the body of the neuron. The axon is the output channel, the extension of soma, and carries nerve impulses from soma to other neurons. The origin and the end of the axon are called hillock and bouton respectively. The synapses are areas of electro chemical contact between neurons.

The ANN is to simulate a biological neural network. So their structures are similar to each other, namely, a basic ANN model is composed of a large number of neurons, linked to each other with connection weights and each neuron has multiple inputs and single output.

Neural networks have just started to become popular but their research are not new. Their history dates back more than 40 years. Work in neural network is classified by DARPA [31] into three areas, as shown in the following page.

Early Work 1940-1960 Fundamental Concept	McCulloch & Pitts Hebb Farly & Clark Rosenblatt Steinbuch,Tylor	-Boolean Logic -Synaptic Leaning Rule -First Simulation -Perceptrons -Associative Memories
Transition 1960-1980 Theoretical foundations	Widrow & Hoff Albus Anderson Von Der Malsburg Fukushima Grossberg	-LMS Algorithm -Cerebellum Model (CMAC) -Linear Associative -Competitive Learning -ART,BCS
Resurgence 1980- Theory Biology Computers	Kohonen Feldman & Ballard Hopfield Reilly,Cooper et al Hinton & Sejnowski Rumelhart & McClelland EdelMan, Reek	-Feature Map -Connectionist Model -Associative Memory Theory -RCE -Bolzman Machine -Back Propagation -PDP Books -Drawin III

2.2.2 Neural Network Models

There is no unique way to classify the neural network models, since these models contain different methods of learning, structures and functions. A simple classification of ANN model from model is shown in *Figure 2.3*

The characteristics of ANN models have been surveyed and a brief discussed is presented below. A complete discussion on each model is described in [31,32].

1. Feedback vs. Feedforward

   Figure 2.4 shows the architecture of feedforward and feedback ANN model. In brief, if no Process Units(PU) output is dependent on any of its previous values, then the network is said to be feedforward. But, in the feedback network, PU's output will be connected with its input.

2. Linear vs. Nonlinear

   In both linear and nonlinear models, the receiving PU takes into account the rates at which PUs are sent, multiplies them by their corresponding weights and sums them up. The difference between these two models lies in the relationship between the output of PU and the summation.

   Linear model means the output of PU is a linear function of summation and nonlinear model's output is a nonlinear function of summation.

3. Association vs. Evaluation

   There are two types of ANN input/output architectures: association and

evaluation [33].

In association: ANN takes an input and tries to associate it with a previously defined output category.

In evaluation: ANN takes each input and produces an evaluation of that input. If it is the transition between two states that needs to be evaluated, the network is supplied with before and after situations as part of its input. It rates this pair of state.

4. Learning Paradigms

ANN can be classified by the learning paradigms, because these learning paradigms provide a good idea of the potential capabilities of the neural network technology [35]. These learning paradigms will be discussed in the next section.

5. Fully Connected vs. Sparsely Connected

If PUs are connected to all other PUs, we call it a fully connected network. In the sparsely connected network, the PUs are only connected to few others.

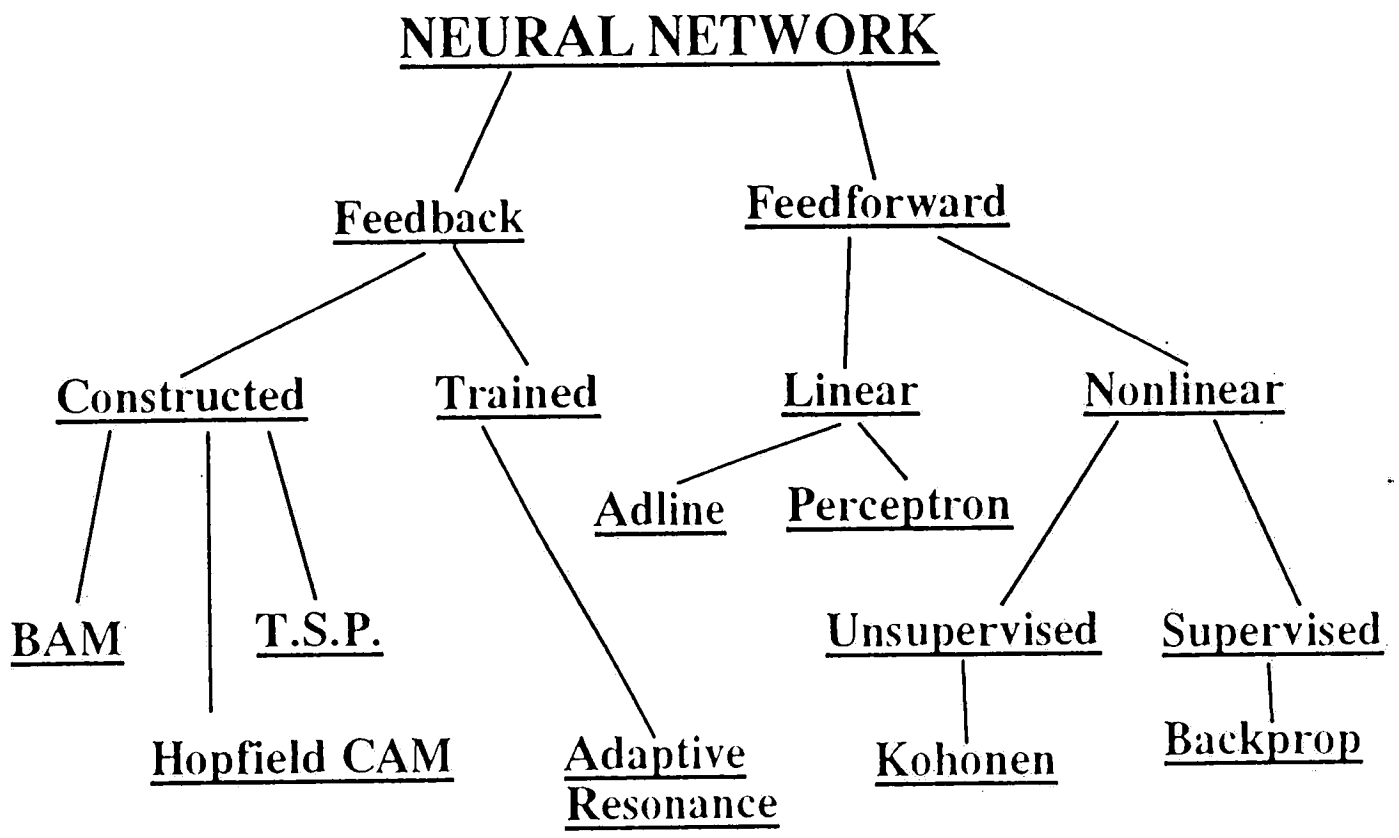

Figure 2.3 Neural Network Models

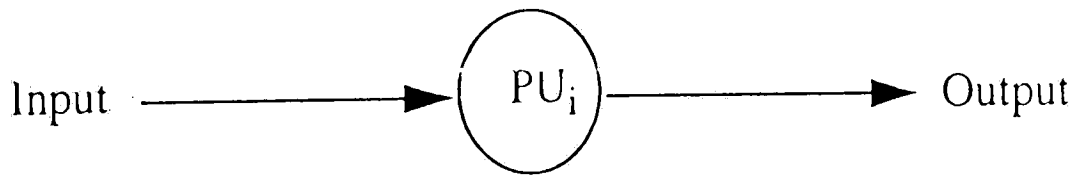

(a) Feed Forward Network

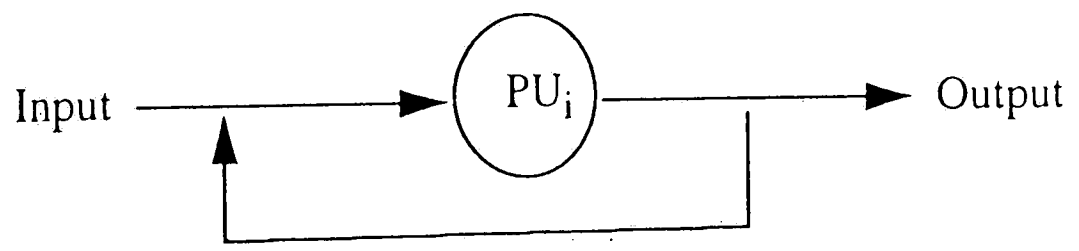

(b) Feedback Network

Figure 2.4 Feed Forward and Feed Back Network

2.2.3 Learning Algorithm

The learning rule is the heart of a neural network. It defines how to change the weights in response to a given input/output pair. From the previous research [31,34], three types of learning rule exist: supervised learning, unsupervised learning and self-supervised learning.

In this section, six well-known learning rules such as Hebb's Rule, Delta rule, Gradient Decent rule and Back Propagation rule will be briefly discussed.

1. Hebb Rule

This rule is one of the first and certainly the best-known. The basic idea of Hebb rule is: If PU a_i receives an input from another PU b_j, and if both are highly active, the weight w_{ij} from a_i to b_j should be strengthened. Hebbian rule is usually expressed as follows

$$\nabla W_{i,j} = \eta a_i b_j$$

Where η is the learning rate, which is the measure of speed of the convergence of the initial weight pattern to the ideal pattern

2. Delta Rule

The Delta rule, also called Least Mean Squared (LMS), was developed by Bernard Widrow and Ted Hoff. The network itself was called ADALINE, a shortened for of ADAptive LINear Element. This rule states that if there is a difference between the actual and the desired output during training, then the weights are changed to reduce the

difference. The amount of change to the weight is obtained by multiplying the error of the outputs with the values of the inputs and the learning rate is:

$$w_{ij} = (t_i - a_i)^* b_j$$

Where t_i is the desired target

3. Gradient Descent Rule

Gradient Descent rule minimizes the error measure E by a procedure that modifies the connected weights by an amount proportional to dE/ $dW_{i,j,}$:

$$\Delta W_{i,j} = \eta \frac{dE}{dW_{i,j}}$$

The drawbacks of this approach are: 1. It converges very slowly. 2. It can not provide a global minimum, that is, it just finds a local minimum.

4. Back Propagation Rule

This is a supervised learning rule in which training runs forward through the network layers first, then the errors are propagated backwards, and the connected weights are updated in order to reduce the errors. So far this rule is commonly used in neural network. The Back Propagation

algorithm is shown as follows:

1. Initialize the weights and the thresholds to small random values.

2. Present input and desired outputs.

3.Calculate the actual outputs by sigmoid function.

4. Adapt weights.

Use a recursive algorithm starting at the output nodes and working back to the first hidden layer.

Adjust weights by

$$W_{i,j}(t+1) = W_{i,j}(t) + \eta \delta_j x'_i$$

where: W_{ij} (t): the weight from hidden node i or from an input

to node j at time t.

x'_i = either the output of node i or is an input

η = learning rate

δ_j = an error term for node j

If node j is an output node, then

$\delta_j = y_j (1 - y_j) (d_j - y_j)$

where d_j: the desired output of node j

y_j: the actual output

If node j is an internal hidden node, then

$$\delta_j = x_i' (1 - x_i') \Sigma \delta_k w_{jk}$$

where: k = over all nodes in the layers above node j

5. Repeat by going to step 2.

2.2.4. Neural Network Applications

As pointed out in [34,35] Neural network has been applied to areas like pattern recognition, expert system, speech processing, decision support system, neural modeling and natural language processing.

By using a combination of rule-base and modeling technique, Chryssolouris and Gullot proposed an approach to the selection of process parameters[36]. Three modeling techniques, namely, multiple regression, GMDH and neural network were utilized in the research. The best results were obtained from the GMDH and neural network with dimension such as 5x20x1.

A scheme presented by Rangwala and Dornfeld utilized a feedforward neural network for the learning and synthesis task[37-39]. Back propagation was then used as a training algorithm on the model to set up a multi-layer for monitoring tool wear in turning operation[40]. A multiple sensor scheme utilizing cutting force and acoustic emission information was also developed. The network showed a high convergent rate and ability to integrate and generalize information from different sources with 95% accuracy in a turning operation. Steep descent was used to minimize the training error in back propagation algorithm. Inputs to the network were defined as multichannel

autoregressive (AR) series model parameters and power spectrum amplitude. Following observations were obtained:

1. By applying the multichannel AR time series model with the neural network structure for learning the characteristics of the signals from multiple sensors which depend on the state of cutting tool, tool wear can be effectively detected.

2. The system can be applied to a wide range of cutting conditions. This feature make it possible to significantly reduce in-plant calibration time.

3. Optimal condition and efficiency of the tool wear detection system will be ensured by carefully selecting the network parameters.

In [41], an intelligent monitoring and diagnostic system for quality assurance based on the integration of multiple sensors like cutting force, acoustic emission and spindle vibration via multi-layer neural network in conjunction with an expert system has been developed. The surface finish and bore tolerance in circular end milling of 6061-T6 aluminum workpiece was obtained. RMS of the horizontal resultant force, of spindle acceleration and acoustic emission event magnitude were found as the best sensor feature that could be correlated with surface finish and bore tolerance. The effect of different sensor fusion, network structure and the number of data points used in the training set on the network performance were evaluated.

Chapter 3

Experiment and The Neural Network Modeling of Grinding Process

The experiment pertaining to the creep feed grinding of two types of superalloys is discussed in Section 3.1. The machine setup and different working conditions are also included in the discussion. Section 3.2 focuses on the neural network model obtained from the training procedure. The results of the experiment as well as the neural network performance are discussed in section 3.3

3.1 Data Collection

The experiments were carried out by using CBN wheels measuring 17.78 cm in diameter and 0.317 cm in width. The work materials used in the experiment are Ti- 6Al-4V and Inconel 718 of dimension 6.99 cm x 2.54 cm x 2.54 cm. A JUNG creep feed grinder was used to perform the grinding test. A special fixture was designed to hold the workpiece on top of the KISTLER 9257 three component dynamometer. ADCOOL #3 was used as a coolant at a flow rate of 20 gallons/min. Wheel speed was maintained at 20 m/s. A brake controlled truing device was used to true the CBN wheel. This was followed by dressing with SiC sticks. Though the dressing conditions can't be claimed to be identical it can be assumed to be within experimental error. The force components were sampled at intervals of 50,100 or 200 ms depending on the feed rate of the work piece. Power and force were obtained from the amplifier reading. These digitized data were stored on floppy disks for the later pro-

cessing. Surface finish values for the ground surfaces were measured by PERTHERN profilometer. The working conditions are as follows:

CBN Wheels

Bond	Mesh size	Concentration
Resin	120/140	125
Vitrify	150	180

Feed Rate: 25 mm/min, 50 mm/min, 100 mm/min

Depth of Cut: 0.625 mm, 1.25 mm, 1.875 mm

Work Material: Ti-6Al-4V, Inconel 718

3.2 Network Model of The Process

Wheel bond type, feed rate and depth of cut comprise the input vector of the network. The output vector from the network consists of power(P), force(Fn) and surface finish(Ra). Twelve out of eighteen data points are presented as training set. The rest of the data points were used to verify the convergence of the network. The networks with one to six hidden nodes were trained to investigate the effect of the number of hidden nodes to the overall performance. The one which gave the best result was selected to formulate the model for the optimization of the grinding process. The system configuration is shown in *Figure 3.1*

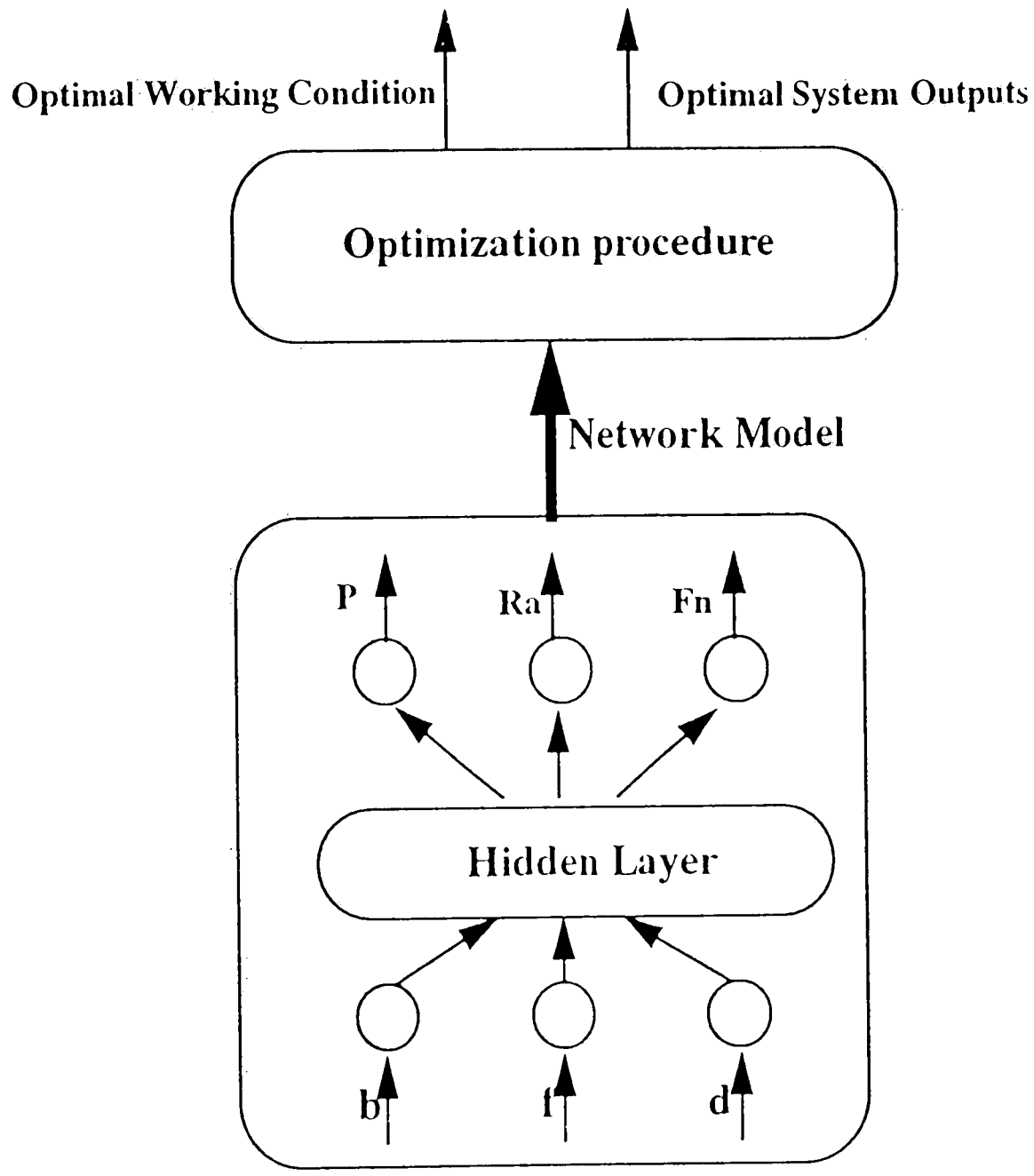

Figure 3.1 Neural Network Model of Grinding process

3.3 Experiment Result and Network Performance

The convergence of the networks was observed during the training process. Faster convergence was achieved with more nodes in the hidden layer. But this is not the best rule to guarantee the convergence. No obvious difference in the convergence among the networks was observed after increasing the node number to three.

Figure 3.2 shows the performance of the networks trained for Ti-6Al-4V. The network with two nodes in the hidden layer gave the least error and it was selected to formulate the model. Although this network didn't provide the fastest convergence, it provided the minimum least square error. *Figure 3.3* is the performance diagram for Inconel 718. Network with only one hidden node was selected due to the least error.

Figures 3.4 and *3.5* show the forces and surface finishes versus feed rate and depth of cut for grinding Ti-6Al-4V and Inconel 718, respectively. For both materials, an obvious increase in force is observed by increasing the feed rate and depth of cut. Although not as prominent as that of the force, a lager value for surface finish was also observed by increasing the feed rate and depth of cut.

Based on *Figure 3.4* and the results of the experiment, comparison of the performance between vitrified and resinoid wheels can be made when cutting Ti-6Al-4V:

•Vitrified wheel requires less normal force and power than resinoid wheel at higher feed rate.

•No distinction can be made between the performance of vitrified and resinoid wheel as far as surface finish is concerned.

•Lower power and force were required for vitrified wheel especially at higher depth of cut.

Figure 3.5 shows the corresponding information Inconel 718. Based on this figure and the results from experiment, following observations are made:

•Resinoid wheel requires less force than the vitrified wheel. The higher the depth of cut and feed rate the more force is required for vitrified wheel than for resinoid wheel.

•Vitrified wheel generated better surface finish at higher feed rate and depth of cut.

•Resinoid wheel also had the advantage over vitrified wheel in consuming less power for the same working conditions.

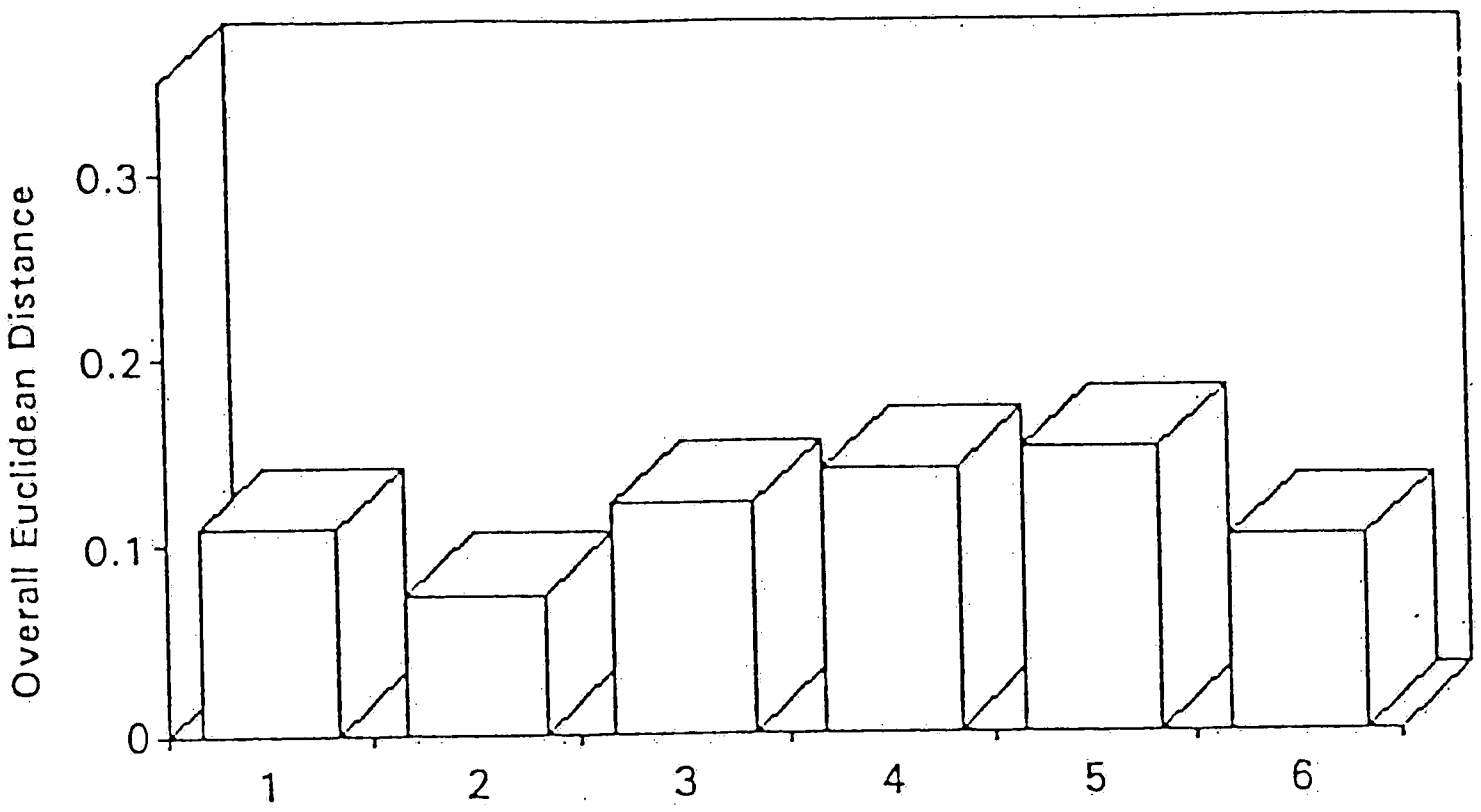

Figure 3.2 Network Performance for Ti-6Al-4V

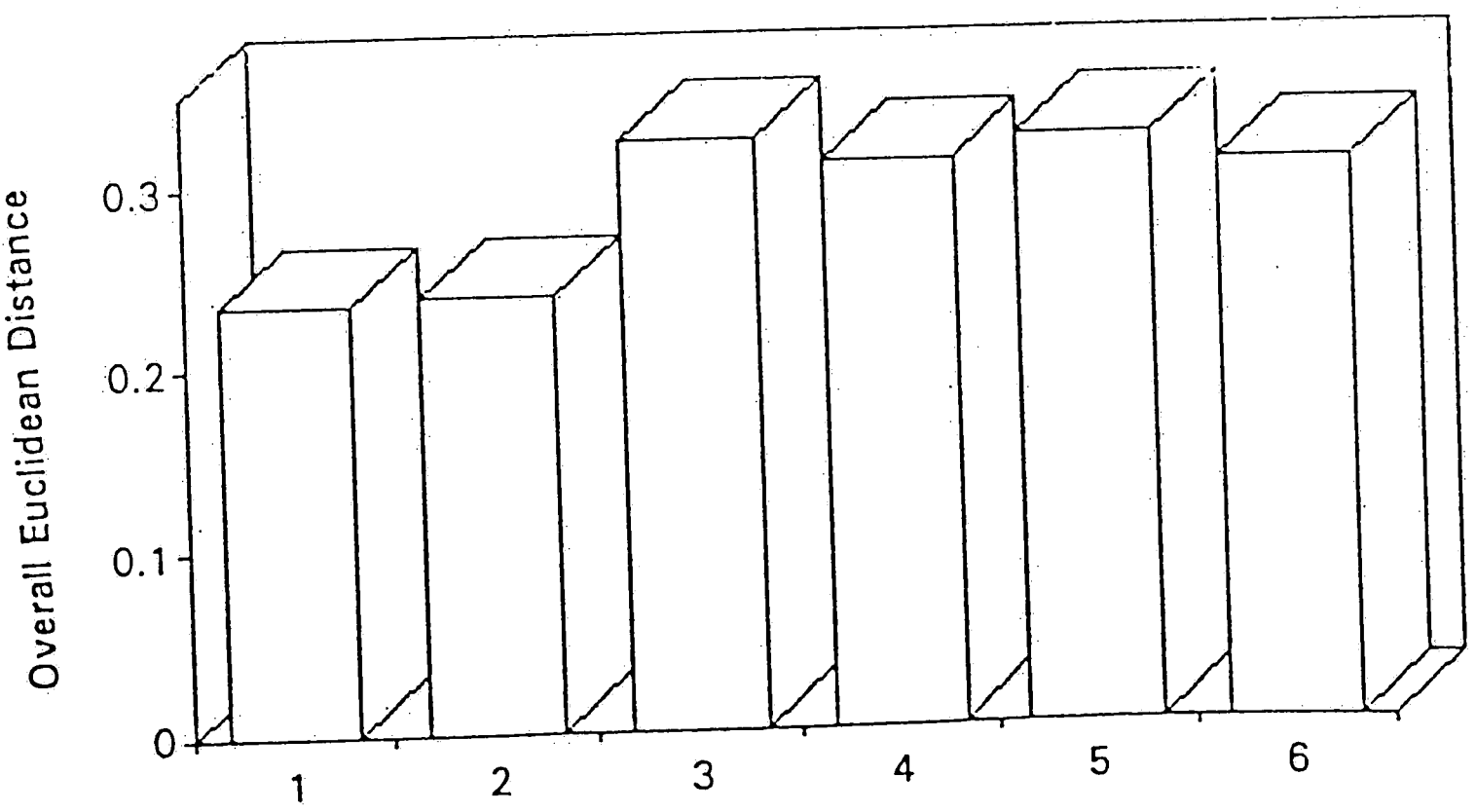

Figure 3.3. Network Performance for Inconel 718

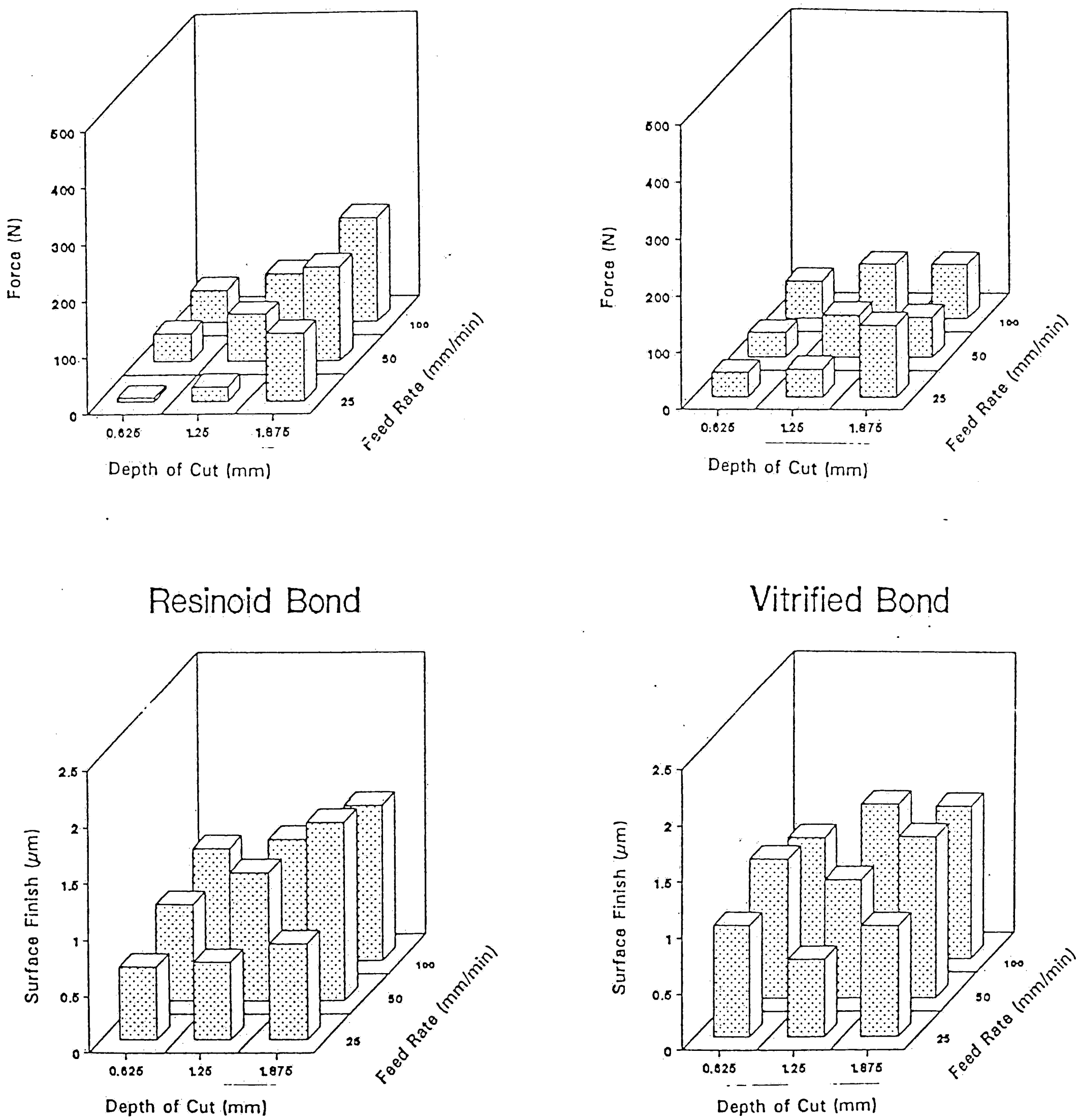

Figure 3.4 Force and Surface Finish for Ti-6Al-4V

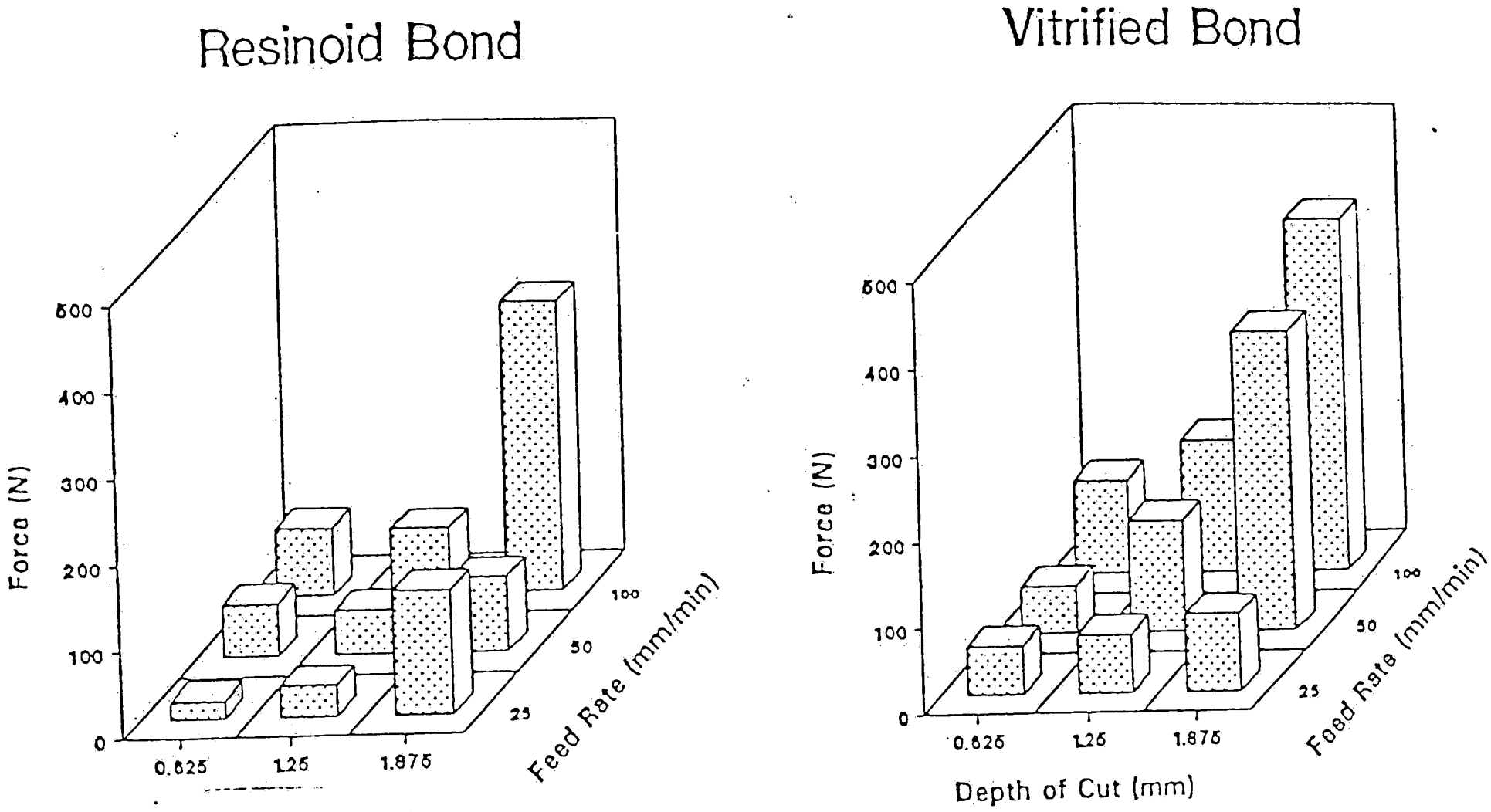

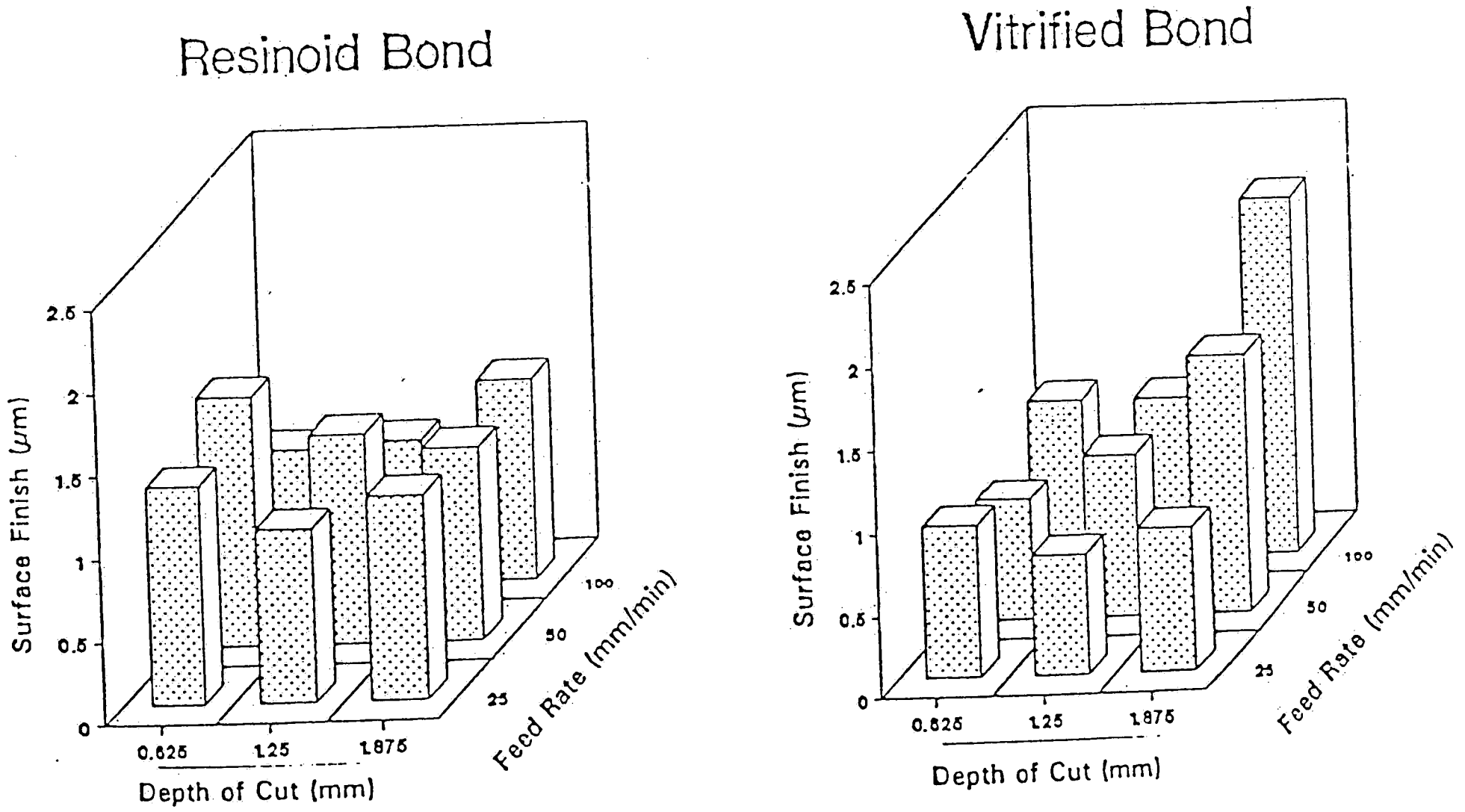

Figure 3.5 Force and Surface Finish for Inconel 718

Chapter 4

Grinding Process Optimization

The optimization of the neural network models obtained in chapter three is discussed here. Section 4.1 is pertaining to the optimization methodology that was utilized to solve the multi-objective problem. Section 4.2 presents the formulated optimization model. Section 4.3 concludes the chapter with the discussion of the results obtained from the optimization procedure.

4.1 Optimization Methodology

The objectives of a multi-objective optimization problem can be combined into a single function by assigning a weight for each objective.The optimization can then be achieved by parametric variation of the weights assigned to each objective and he set of non-dominated solution can be approximated. The procedure begins by optimizing each objective individually. After each objective is optimized, systematic variation in the weight is carried out. Each weight is varied from zero to some upper bound using a predetermined step size. The method presented by Cohen[42] is utilized to check the inferiority of the alternate optima, which might occur when one or more weights are set to zero.

The branch and bound method is used to solve the single objective nonlinear mixed integer problems. Based on[43] the most fractional integer variable is selected as the branching variable and the node with the lowest bound is selected as the branching node. An algorithm based on the Generalized Reduced Gradient (GRG) method is used to solve the intermediate nonlinear continuous problem.

4.2 Problem Formulation

The output of the sigmoid transfer function utilized in the network models was constrained to give a value between zero and one which was indeed performing a normalization of the outputs. The normalized optimization model from neural network is formulated as follows:

Multi-Objective Optimization From Neural Network Model

$$Min = W_1 \times P + W_2 Ra + W_3 \times Fn - W_4 \times MRR$$

$$0.333333 < d < 1.0$$

$$0.25 < f < 1.0$$

$$0 < P < UP$$

$$0 < Ra < URa$$

$$0 < Fn < UFn$$

$$P = 1/(1 + exp(-net_{31}))$$

$$Ra = 1/(1 + exp(-net_{32}))$$

$$Fn = 1/(1 + exp(-net_{33}))$$

$$net_{31} = out_{21} \times W_{211} + out_{22} \times W_{221} + t_{31}$$

$$net_{32} = out_{21} \times W_{212} + out_{22} \times W_{222} + t_{32}$$

$$net_{33} = out_{21} \times W_{213} + out_{22} \times W_{223} + t_{33}$$

$$out_{21} = 1/(1 + exp(-net_{21}))$$

$$out_{22} = 1/(1 + exp(-net_{22}))$$

$$net_{21} = out_{11} \times W_{111} + out_{12} \times W_{121} + out_{13} \times W_{131} + t_{21}$$

$$net_{22} = out_{11} \times W_{112} + out_{12} \times W_{122} + out_{13} \times W_{132} + t_{22}$$

$$out_{11} = 1/(1 + exp(-(b + t_{11})))$$

$$out_{12} = 1/(1 + exp(-(d + t_{12})))$$

$$out_{13} = 1/(1 + exp(-(f + t_{13})))$$

where

W_1: weight for power;, W_2: weight for surface finish (Ra)
W_3: weight for normal force (Fn), W_4: weight for MRR
UP: upper bound for power
URa:upper bound for surface finish,UFn:upper bound for force
net_{ij}: net input of the jth node in layer i
out_{ij}: output of the jth node in layer i
t_{ij}: threshold of the jth value in layer i
W_{ijk}: the kth element of weight set for the jth node in layer i
out_{22},net_{22},t_{22},W_{221},W_{222},W_{223} are set to 0 in the network for Inconel 718 and 1 for Ti-6Al-4V

4.3 Optimal System Condition

The upper bound settings for P, Ra and Fn for Ti-6-Al-4V were set at 3.5 KW,1.3 μm and 95N, respectively. The maximum feed rate and depth of cut are set at 100 mm/min and 1.875 mm. Optimization strategies for resinoid and vitrified wheel are provided in *Table 4.1* and *4.2* respectively.

TABLE 4.1 Result of optimization study for resinoid wheel (Ti-6Al-4V)

W_1	W_2	W_3	W_4	P	Ra	Fn	MRR	d	f
1	0	0	0	1.44	0.730	29.11	15.625	0.625	25
0	1	0	0	1.44	0.730	29.11	15.625	0.625	25
0	0	1	0	1.44	0.730	29.11	15.625	0.625	25
0	0	0	1	3.50	1.179	80.43	78.528	1.827	42.96
1	1	1	1	1.44	0.730	29.11	15.625	0.625	25
1	1	1	2	1.44	0.730	29.11	15.625	0.625	25
1	1	1	3	1.73	0.750	38.61	23.916	0.625	38.26

TABLE 4.2 Result of optimization study for vitrified wheel (Ti-6Al-4V)

W_1	W_2	W_3	W_4	P	Ra	Fn	MRR	d	f
1	0	0	0	1.69	0.864	31.52	15.625	0.625	25
0	1	0	0	1.69	0.864	31.52	15.625	0.625	25
0	0	1	0	1.69	0.864	31.52	15.625	0.625	25
0	0	0	1	3.50	1.207	78.78	74.813	1.875	39.90
1	1	1	1	1.69	0.864	31.52	15.625	0.625	25
1	1	1	2	1.69	0.864	31.52	15.625	0.625	25
1	1	1	3	3.50	1.195	78.78	74.831	1.875	39.91

According to the above tables, minimum power(P), surface finish(Ra) and force(Fn) for resinoid wheel can be achieved simultaneously by setting W_4 to a value less than three. The maximum MRR for resinoid wheel can be achieved by setting the feed rate of 39.91 mm/min and depth of cut of 1.875 mm under the current constraint.

The minimum power(P), surface finish(Ra) and force(Fn) for vitrified wheel can also be achieved simultaneously by setting W4 to a value less than 3. A 39.91 mm/min and 1.875 mm depth of cut can help in achieving maximum MRR.

When setting feed rate equal to 25 mm/min and depth of cut to 0.625 mm which is the condition when both types of wheels achieve the optimal power(P), surface finish(Ra) and force(Fn), resinoid wheel performs better than vitrified wheel. If the MRR is the major concern under the current constraint, the suggestion will be to choose resinoid wheel.

A value path diagram is drawn to facilitate the visualization of the trade-off between the objectives and is shown in *Figure 4.1*.The line number with the associated weight set is shown as follows:

W_1	W_2	W_3	W_4	Line Number:
1	0	0	0	1
0	1	0	0	2
0	0	1	0	3
0	0	0	1	4
1	1	1	1	5
1	1	1	2	6
1	1	1	3	7

The upper bounds for P, Ra and Fn are set at 2.68 KW,1.29 μm and 328 N for Inconel 718. The maximum feed rate and depth of cut are set at 100 mm/min and 1.875 mm. Optimization strategies for resinoid and vitrified wheel are provided in *Table 4.3* and *4.4* respectively.

TABLE 4.3 Result of optimization study for resinoid wheel (Inconel 718)

W_1	W_2	W_3	W_4	P	Ra	Fn	MRR	d	f
1	0	0	0	1.64	1.004	71.30	15.625	0.625	25
0	1	0	0	1.64	1.004	71.30	15.625	0.625	25
0	0	1	0	1.64	1.004	71.30	15.625	0.625	25
0	0	0	1	2.68	1.078	113.58	146.144	1.773	82.42
1	1	1	1	2.02	1.031	86.14	125.425	1.623	77.28
1	1	1	2	2.42	1.06	102.35	140.012	1.729	80.96
1	1	1	3	2.68	1.078	113.58	146.144	1.773	82.42

TABLE 4.4 Result of optimization study for vitrified wheel (Inconel 718)

W_1	W_2	W_3	W_4	P	Ra	Fn	MRR	d	f
1	0	0	0	1.65	0.527	71.39	15.625	0.625	25
0	1	0	0	1.65	0.527	71.39	15.625	0.625	25
0	0	1	0	1.65	0.527	71.39	15.625	0.625	25
0	0	0	1	2.68	1.078	113.60	94.550	1.384	68.32
1	1	1	1	1.94	1.025	82.96	74.115	1.209	61.25
1	1	1	2	2.26	1.049	95.96	85.887	1.312	65.46
1	1	1	3	2.59	1.072	109.68	92.982	1.371	67.81

It can be observed from the tables, by omitting the importance of MRR, optimal values of power(P), surface finish(Ra) and force(Fn) for the resinoid wheel can be obtained simultaneously by operating feed rate and depth of cut at respectively 0.625 mm and 25 mm/min. The maximum MRR for resinoid wheel can be achieved by setting the feed rate at 68.32 mm/min and depth of cut at 1.384 mm under the current constraint.

The minimum power(P), surface finish(Ra) and force(Fn) can also be achieved simultaneously with the vitrified wheel. This requires a setting of 0.625 mm depth of cut and 25 mm/min feed rate. Under the current constraints, maximum MRR can be achieved at 1.384 mm depth of cut and 68.32 mm/min feed rate. Again, decision maker can visualize the value path dia-

gram shown in *Figure 4.2* to realize the appropriate optimal combination of working conditions.

Resin

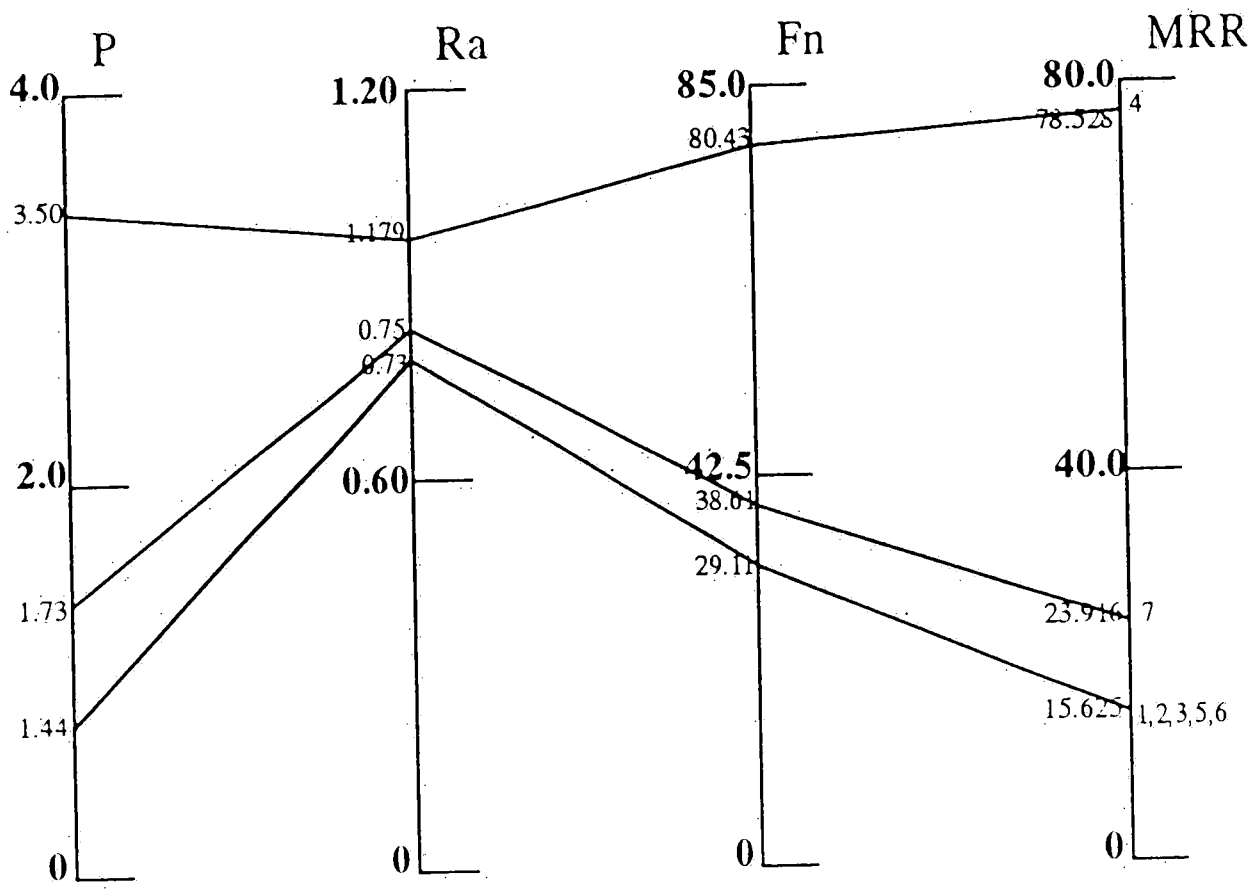

Vitrified

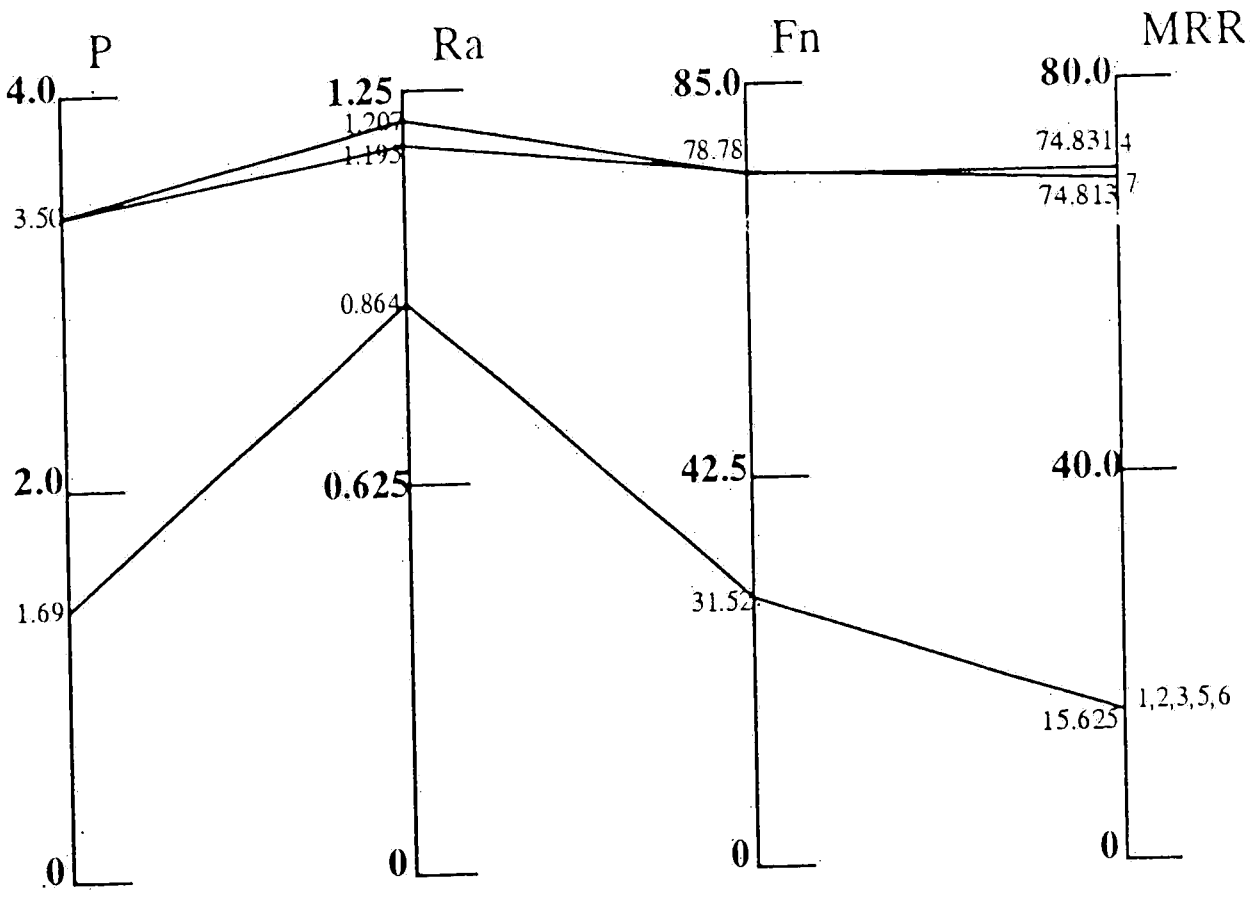

Figure 4.1. Value Path Diagram for T-6Al-4V

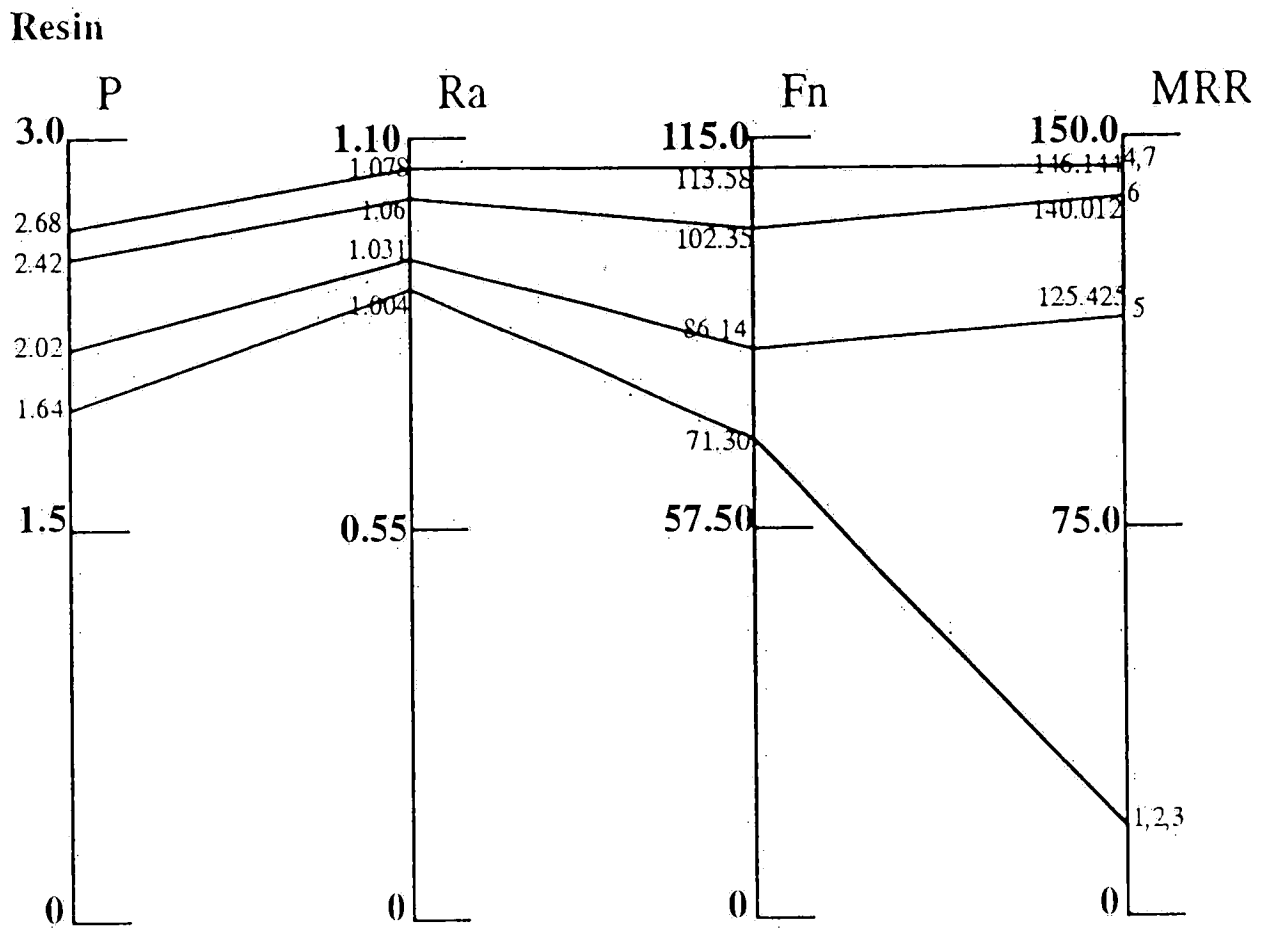

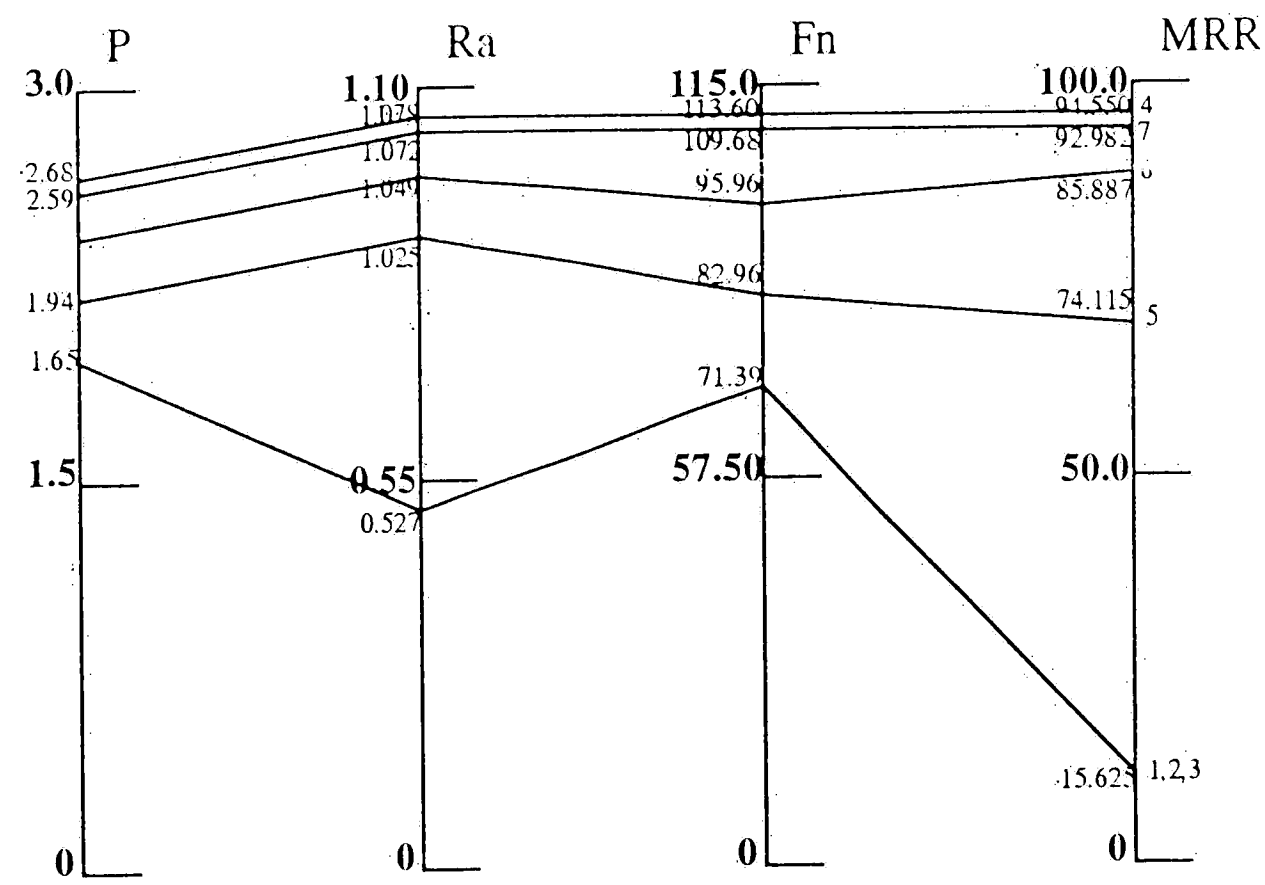

Figure 4.2 Value Path Diagram for Inconel-718

Chapter 5

Modeling Wheel Topography and Wheel Characterization of CBN Wheels

The author believes that an accurate modeling of the interaction between the work-grit will help in the exploration of the grinding process, and in turn will help in controlling and in achieving the optimal strategy for the process. The ideas and the applications presented in this chapter provide new approaches to achieve this goal.

Section 5.1 describes the details pertaining to the wheel profile data acquisition. The equipment and the layout of the data collection device are also presented schematically.

Section 5.2 proposes a new approach (see *Figure 5.1*) for the simulation and modeling of the wheel profile based on the Fractal analysis. Section 5.3 presents the Iterative Function System (IFS) to simulate the CBN wheel profile. Section 5.4 discusses the technique to calculate the dynamic active cutting edges. Section 5.5 utilizes the Markov Chain theory to characterize the wheel profile and to achieve a probabilistic model for the active cutting edges in the cutting zone. Section 5.6 develops a new approach for the modeling of the dynamic interaction in the cutting zone by Queueing theory.

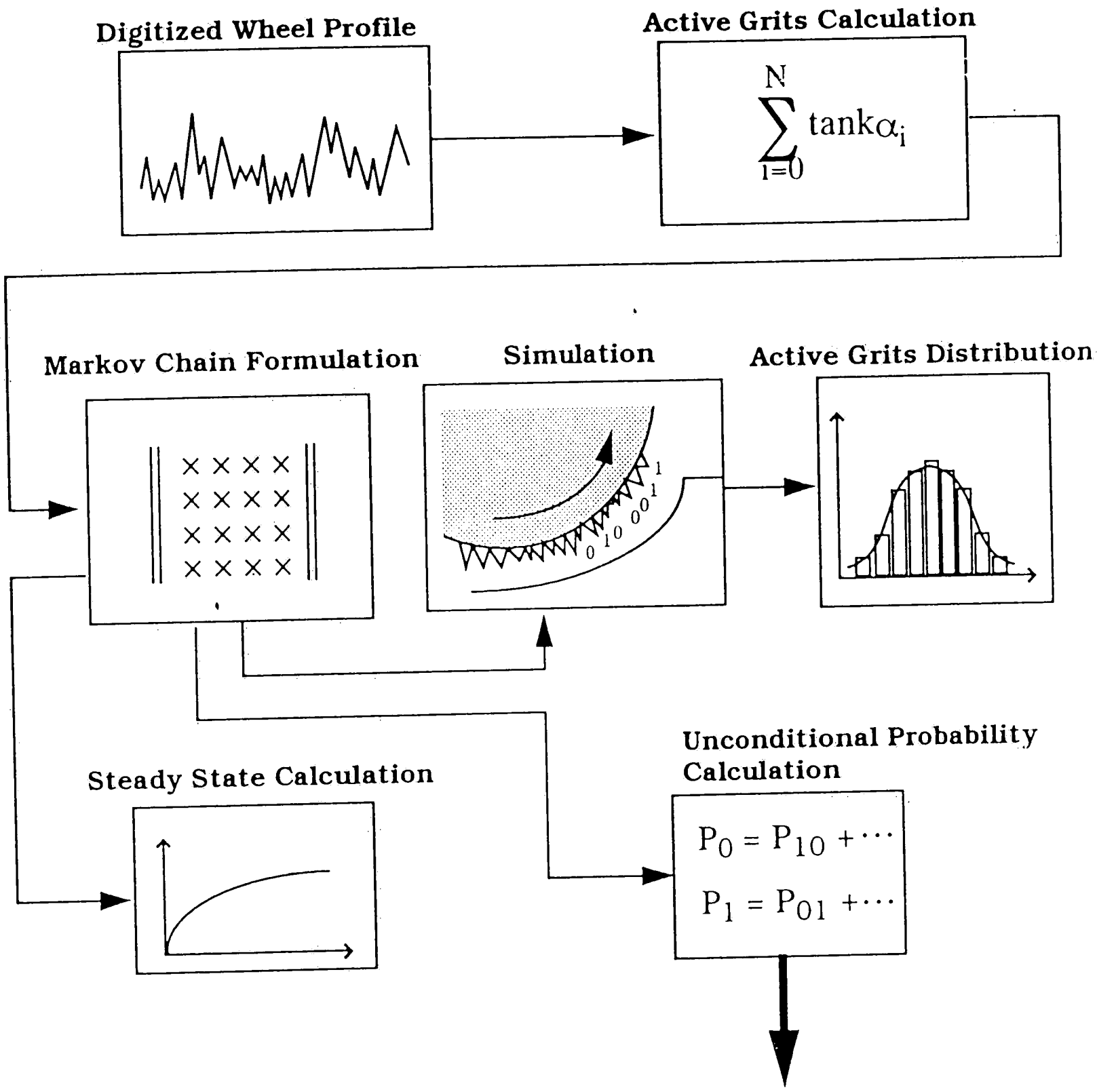

Figure 5.1 Modeling the Dynamics of Grinding Process

5.1 Data Collection

For the purpose of analyzing the geometric attributes and the dynamic cutting events along the wheel circumference, measurements were made parallel to the cutting direction on the wheel. *Figure 5.2* shows the collection system.

In *Figure 5.2*, the first computer was used to control the speed and the direction of the step motor. The program on the computer was designed in a way that the first motor will step 400 times to complete one rotation. The overall gear ratio is 969 which results in a 387600 resolution for the system. The stylus was fixed as wheel was rotating. The magnitude of peaks and valleys on the wheel was then fed into S5P profilometer via the stylus. Norland 3001 then received the signals from the profilometer by checking the data line at a certain interval which was set based on a specific resolution requirement. The data was then sent to the second computer and transformed into ASCII format to facilitate further processing.

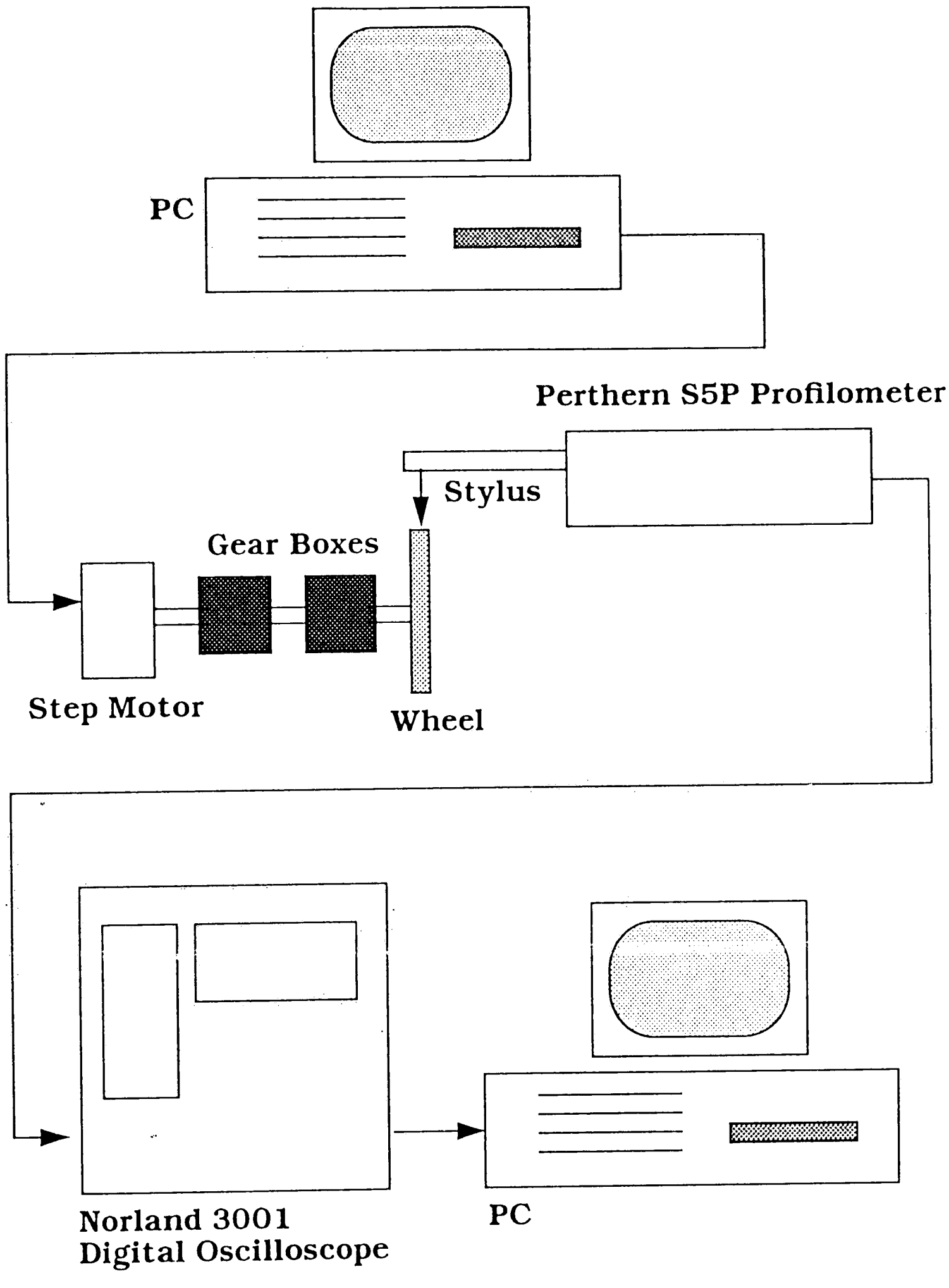

Figure 5.2 Wheel Profile Data Acquisition System

5.2 Fractal and Fractal Dimension

A mathematical definition of fractal is provided in[44] which states that a fractal is located in the space whose points are the compact subsets of a complete metric space. Mandelbrot (1986) proposed a definition on fractal as follows:

"A fractal is a shape made of parts similar to the whole in some way".

An object is said to be a fractal, or exhibit fractal behavior over a range of scales of observations, if, over that range, the object demonstrates self-similarity. A fern showed in *Figure 5.3* exemplifies the similarity. The pattern of the entire picture in *Figure 5.3* is a fern. Focus on any portion of the original picture and magnify it to a certain degree, we can still get the same pattern which is a fern. The procedure can be carried out recursively and infinitely and each time we can associate this with the original picture. This phenomenon also occurs in natural object geometry.

Fractal dimension [25] is the most important factor to characterize a fractal. The fractal dimension has the following property:

$$N(\delta) \propto \frac{1}{\delta^{D}} \qquad (1)$$

Where: D is the fractal dimension.

δ is the measuring unit.

N(δ) is the number of δ units required to cover the graph of the fractal

Fractal dimension is invariant under various distortion of the original graph and is independent of the measuring unit used.

Several techniques have been utilized to calculate the fractal dimension, including: the slit-island method[45], the structure function[44] and coastline or compass method[47]. Another approach which is called variation method was developed in[48]. The variation method was shown to be more suitable for the digitized profile data than the above methods and therefore it was chosen to achieve the fractal dimension for the grinding profile.

The variation method was applied to the CBN wheel profile along parallel and perpendicular to the wheel circumference directions. The procedure starts with an initial measuring unit R_1 as the horizontal distance between a specified number of digitized points in the interval R_1. The area of the box was calculated and the box construction repeated for the same R, but incremented by one data point along the trace. The process continues until the opposite end of the curve is reached. The area of the individual box is summed and normalized by dividing by R^2 to yield the number of the boxes N_1 of side R_1 required to cover the profile trace.

The algorithm proceeds in this manner over the entire range of selected measuring unit lengths. The fractal dimension was calculated from the slope of the log-log plot of the N(R) as a function of 1/R. The log-log plots for vitrified and resinoid wheels are shown in *Figure 5.4*. Fractal dimension for each wheel was obtained from calculating the slope of the linear region of the curve. *Table 5.1* shows the results. Compared to the associated surface finish (Ra), the fractal for the coarser wheel reveals higher occupation of the metric space than that of the finer wheel.

TABLE 5.1

	Vitrified Wheel	Resinoid Wheel
Ra (μm)	10.44	12.18
Fractal Dimension (Traverse)	1.115	1.183
Fractal Dimension (Longitude)	1.277	1.332

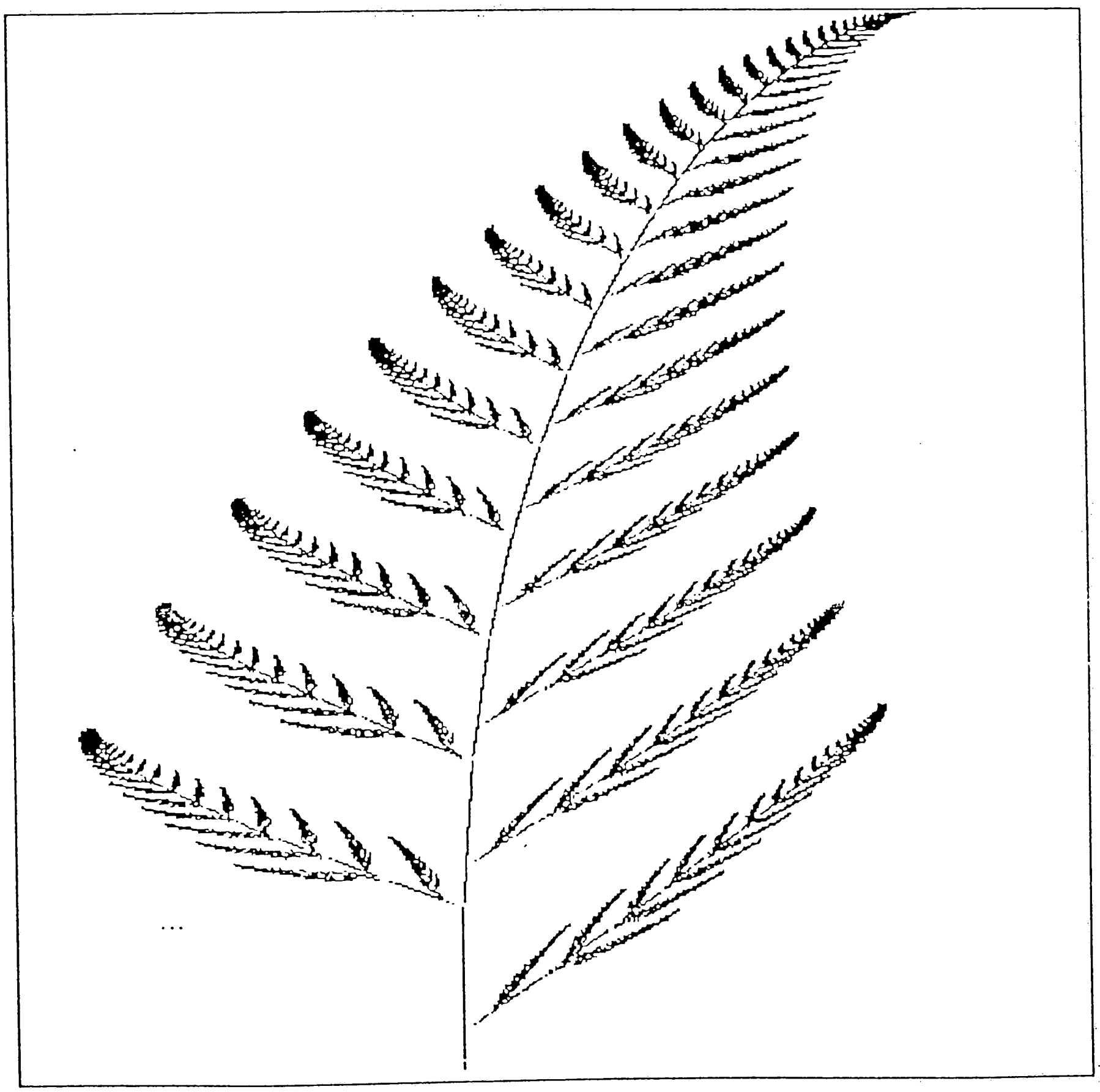

FIg. 5.3 A Fern Generated by Iterative Function

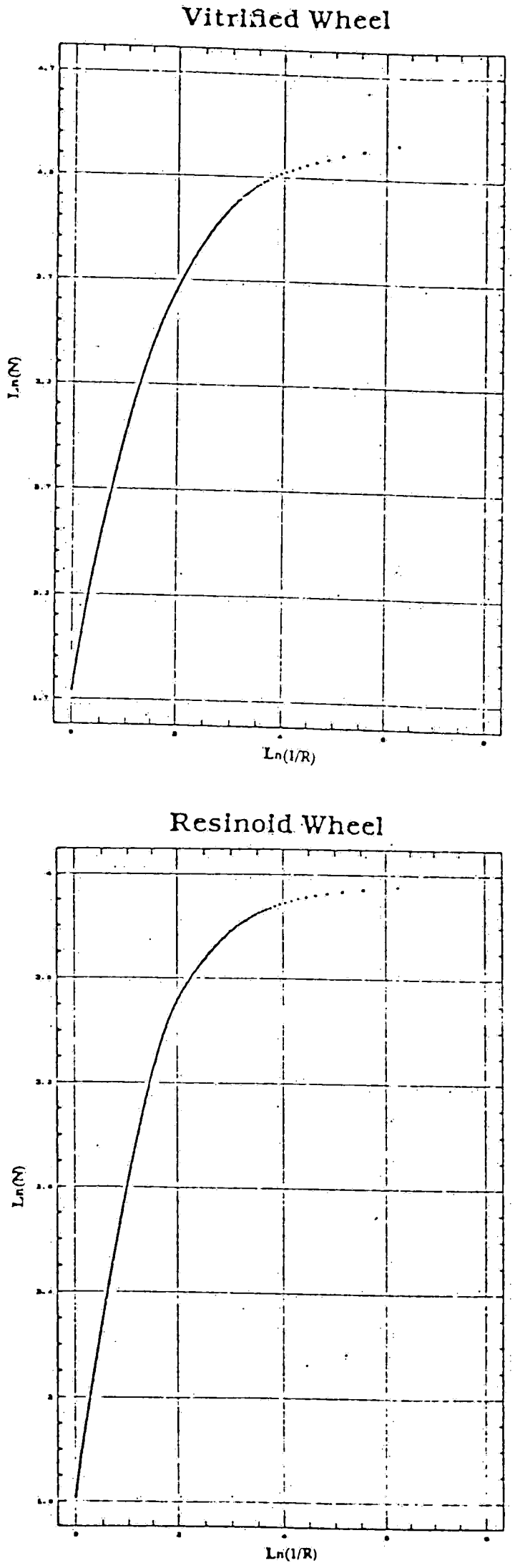

Figure 5.4 The Fractal Dimension of Vitrified and Resinoid Wheels

5.3Wheel Surface Generation by Fractal Interpolation

In view of the natural object geometry, more and more details can be explored by magnifying a portion of the object each time. The magnified portion is similar to the geometric attributes. Examples of the objects that preserve the similarity are ferns, trees, metal surfaces, rocks, projection of cloud surfaces...,etc.

As far as measuring and modeling a curve is concerned, elementary functions, such as trigonometric functions and rational functions have their roots to Euclidean geometry. They share the features that when their graphs are magnified sufficiently, locally they look like straight lines. Moreover, the fractal dimension of those graphs is always one. The above two consequences can be fitted with man-made geometries such as circle and line but won't be the case for the natural objects. It is thus appropriate to investigate the wheel profile by fractal analysis.

Fractal interpolation is a methodology proposed here to model and simulate the wheel profile. It has been proved that the graph generated by fractal interpolation is, in fact, the fractal of the original data [44]. For a set of data $\{(x_i,F_i): i = 0,1,2...N\}$ where N is the number of data points, the methodology is carried out by first defining a set of affine transformations in the form of:

$$w_n \begin{bmatrix} x \\ y \end{bmatrix} = \begin{bmatrix} a_n & 0 \\ c_n & d_n \end{bmatrix} \begin{bmatrix} x \\ y \end{bmatrix} + \begin{bmatrix} e_n \\ f_n \end{bmatrix} \qquad (2)$$

The transformations are contained in the data according to

$$w_n \begin{bmatrix} x_0 \\ F_0 \end{bmatrix} = \begin{bmatrix} x_{n-1} \\ F_{n-1} \end{bmatrix} \tag{3}$$

and

$$w_n \begin{bmatrix} x_N \\ F_N \end{bmatrix} = \begin{bmatrix} x_n \\ F_n \end{bmatrix} \tag{4}$$

for n =1,2,...,N.

The coefficients are calculated according to

$$\begin{aligned} a_n x_0 + e_n &= x_{n-1} \\ a_n x_N + e_n &= x_n \\ c_n x_0 + d_n F_0 + f_n &= F_{n-1} \\ c_n x_N + d_n F_N + f_n &= F_n \end{aligned} \tag{5}$$

The vertical scaling factor d_n must satisfy the following equation to account for fractal dimension of the object:

$$(\frac{1}{N})^{D-1} \sum_{n=1}^{N} |d_n| = 1 \tag{6}$$

After the affine transformation matrices are generated, data points are transformed by randomly selecting one transformation from the transformation set.

A program was implemented to accomplish this methodology and to simulate the wheel profile. The resolution of the simulated result can be increased by adjusting the parameters in the program. The windowing function is also utilized to render the zooming of the fractal curve. The simulated profile along with the corresponding experimental profile for vitrified and resinoid wheels are shown in Figure 5.5. These simulated profile were generated by sampling 1/10 of the original data points and then fed into the program. More simulated profile can be produced by following this procedure with the simulated or experimental data.

Fractal Interpolation for Vitrified Wheel

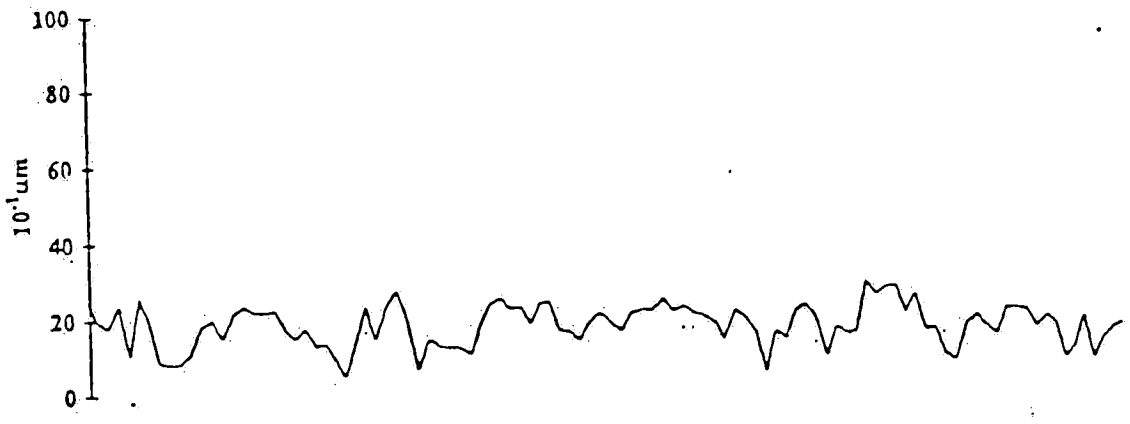

Vitrified Wheel Profile

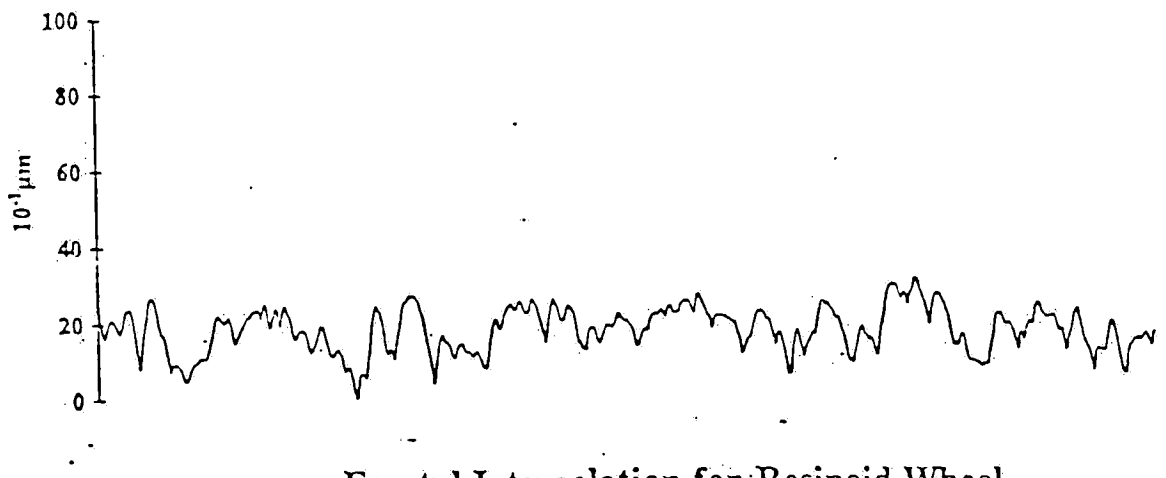

Fractal Interpolation for Resinoid Wheel

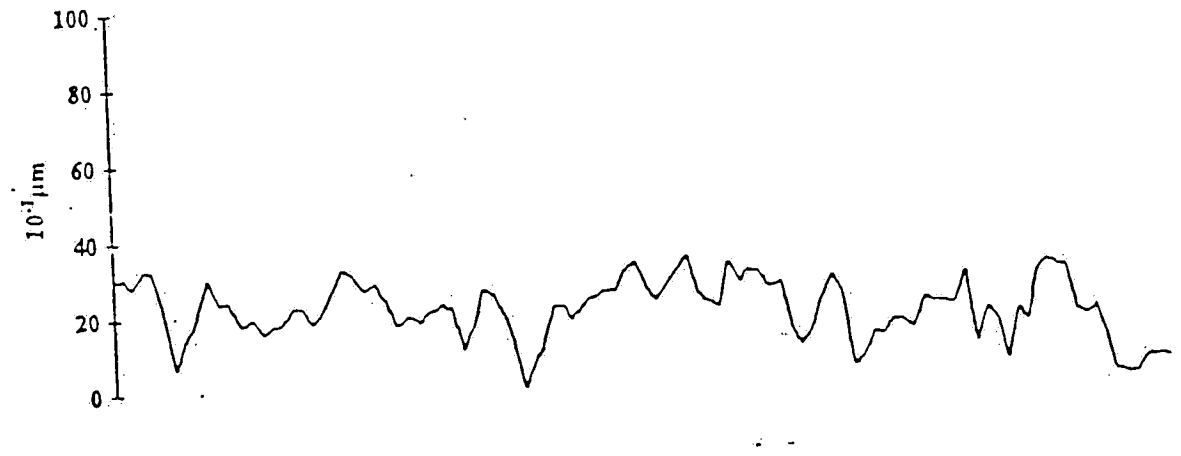

Resinoid Wheel Profile

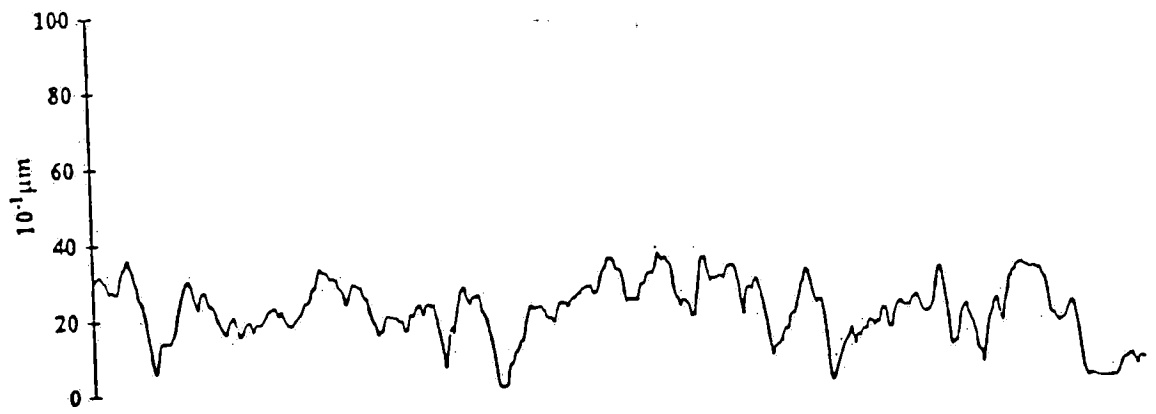

Figure 5.5 Simulated Wheel Profile vs. Experimental Wheel Profile

5.4 Active Cutting Edges Calculation

It's been shown [29] that the undeformed chip thickness for grinding is:

$$h_m = 2L\left(\frac{V_w}{V_s}\right)\left(\frac{a}{d_e}\right)^{\frac{1}{2}} \qquad (7)$$

where h_m = undeformed chip thickness.

L = distance between each cutting point

V_w = feed rate

V_s = wheel speed

a = depth of cut

d_e = effective wheel diameter

The criterion that identifies a cutting point as active is that h_m is strictly greater than zero. Based on this, a program was developed to calculate the number of the active cutting edges and to attach a binary code for each active edge. From the results of the calculation, average number of cutting edges for the vitrified wheel was 19 and 16 for the resinoid wheel. The wheel speed was a dominant factor for the active edges under the current working condition (Vs = 167.64 m/s, Vw = 25 - 100 mm/min and a = 0.625 - 1.875 mm). The number of active cutting edges were the same for every combination of feed rate and depth of cut setting. However, one observation as expected can be made: Due to the higher concentration and finer mesh size, vitrified wheel has more grits than resinoid wheel and therefore a higher number of active cutting edges.

5.5 Markov Chain Characterization of Wheel Profile

A stochastic process is the mathematical abstraction of an empirical process whose development is governed by probabilistic laws. From the point of the mathematical theory of probability, a stochastic process is best defined by a family of a random variables, $\{X(t), t \in T\}$, defined over some index set or parameter space T. The stochastic process can be further classified as discrete or continuous depending on the value that parameter space T can take on. A Markov process is defined as a stochastic process which possesses the memoryless property such that:

$$\begin{aligned} &Pr\{X(t_n) \le x_n \mid X(t_1) = x_1, \ldots, X(t_{n-1}) = x_{n-1}\} \\ &= Pr\{X(t_n) \le x_n \mid X(t_{n-1}) = x_{n-1}\} \end{aligned} \tag{8}$$

The discrete -parameter Markov chain is defined as a Markov process with discrete parameter and discrete state space. The probabilistic structure of the process is determined by the transition matrix which in the form of:

$$\begin{Vmatrix} P_{00} & P_{01} & \cdots & P_{0m} \\ P_{10} & P_{11} & \cdots & P_{1m} \\ & & & \\ P_{m0} & P_{m1} & \cdots & P_{mm} \end{Vmatrix} \tag{9}$$

$$P_{ij} \ge 0, \sum_{j=0}^{m} P_{ij} = 1, i = 0,1,\ldots,m \tag{10}$$

It is appropriate to associate the active cutting edge with binary codes generated from section 5.4 as a discrete Markov chain. A "sample" binary code series is:

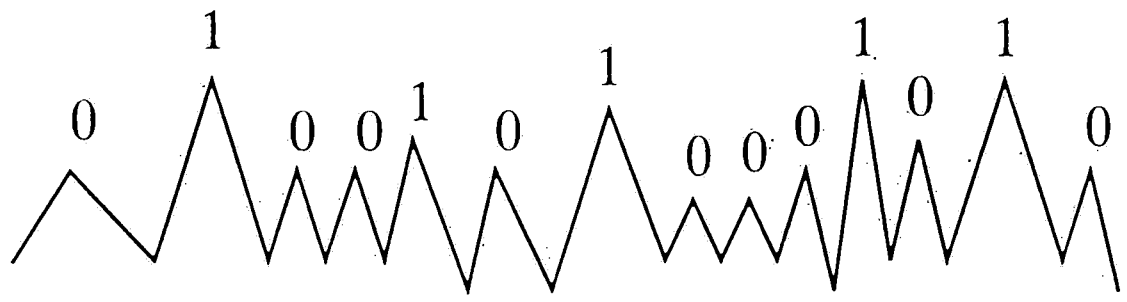

Based on the observation of the experimental series, two major states can be classified for the profile:

1. abrasive grains which account for the cluster of 1's in the series.

2. flat areas between abrasive grains account for the clusters of 0's in the series.

Within each major state, two sub-state can be further recognized: 1 and 0 in 1's and 0's cluster. The state space and parameter space are thus defined as:

$$\text{state space: } \{Xi\},\ Xi = 0 \text{ or } 1$$

$$\text{parameter space: } \{i\},\ i \geq 0,\ i \in Z$$

The form of the resultant second order Markov chain is:

	00	01	10	11
00	X	X	X	X
01	X	X	X	X
10	X	X	X	X
11	X	X	X	X

A program was developed to recognize the major state and then calculate the probability transition matrices for each series. The resultant transition matrices for the vitrified and resinoid wheel are shown below:

Vitrified Wheel

$$\begin{Vmatrix} 0.977003 & 0.000997 & 0 & 0.001999 \\ 1 & 0 & 0 & 0 \\ 0 & 0 & 0.373889 & 0.626111 \\ 0.177217 & 0 & 0.057782 & 0.765001 \end{Vmatrix}$$

Resinoid Wheel

$$\begin{Vmatrix} 0.97901 & 0.000698 & 0 & 0.001401 \\ 1 & 0 & 0 & 0 \\ 0 & 0 & 0.27 & 0.73 \\ 0.167367 & 0 & 0.073799 & 0.758835 \end{Vmatrix}$$

The probability matrices obtained from the previous stage were then taken to conduct the simulation of the active edges in the cutting zone. One thousand times of simulation were conducted for each wheel profile. During every simulation, the total number of active cutting edges were recorded and stored in an ASCII format file.

Table 5.2 shows the statistics of the total number of active edges for each wheel. Both wheels showed very high skewness and unsatisfactory normal plots results. Therefore, distributions that are skew in shape such as lognormal and Gamma distribution are appropriate to fit this data. The Gamma dis-

tribution was chosen because of a good fitting result. Figure 5.6 shows the Gamma probability fitting for vitrified and resinoid wheels. The α and β parameters of the Gamma distribution for vitrified and resinoid wheels are 4.09035, 0.100837 and 2.5558, 0.08355, respectively.

From the statistics, vitrified wheel is expected to have 10 more active edges in the cutting zone on the average than the resinoid wheel. The shape of the distribution for the vitrified wheel is also more centered than that of resinoid wheel. The median, maximum and minimum of the vitrified wheel are higher than that of resinoid wheel, which indicates a prospective higher number of cutting edges. Assuming both wheels are subject to the same load, the resinoid wheel will have a higher unit load than that of the vitrified wheel, and, therefore, higher wheel wear rate and thermal damage. The above properties are due to higher concentration and finer mesh size of the vitrified wheel than that of the resinoid wheel

TABLE 5.2

	Vitrified wheel	Resinoid Wheel
Average	40.564	30.59
Medium	38	24.8411
Geometric Mean	39.72	24,8411
Variance	395.463	326.853
Maximum	183	118
Minimum	4	1
Range	179	117
Skewness	1.2432	0.93846

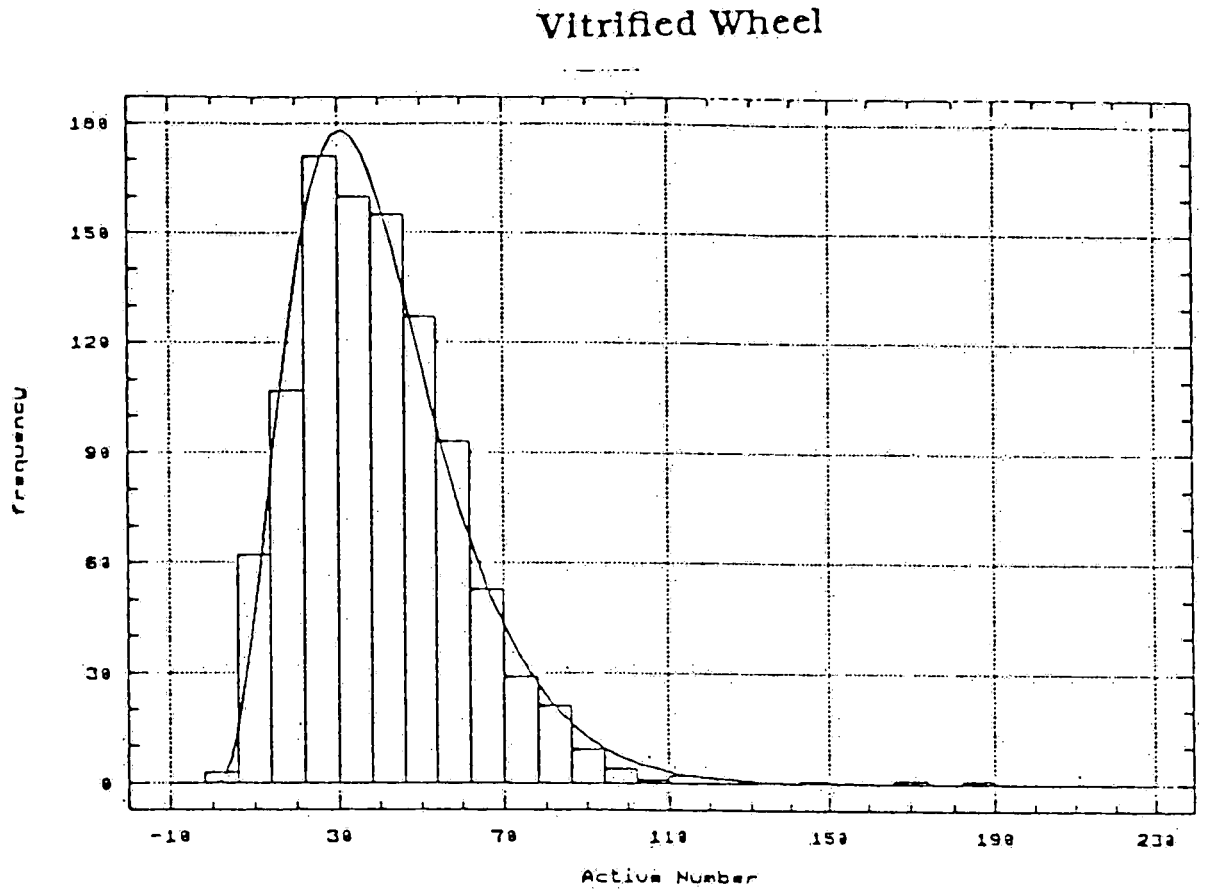

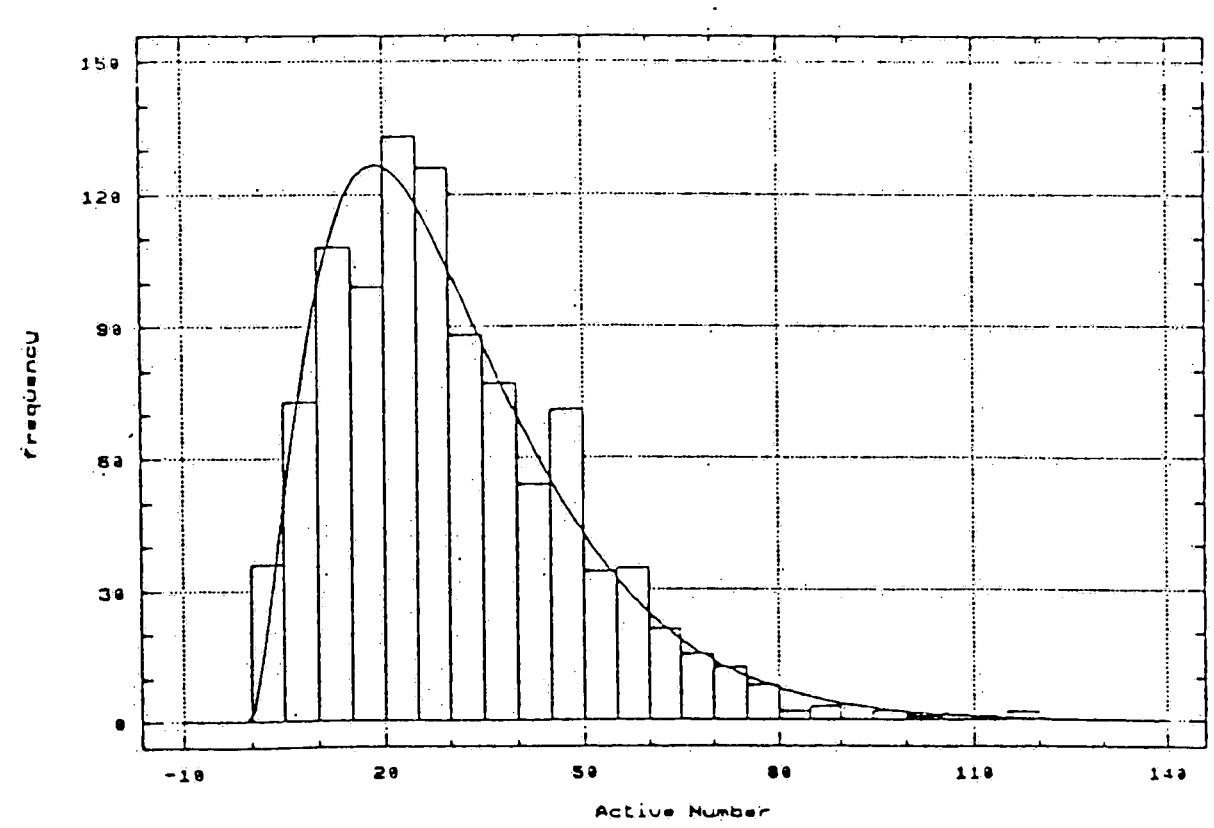

Figure 5.6 Active Cutting edges Distribution

5.6.1 Queueing System for Grinding Process

A queueing system can be described as customers arriving for service, waiting for service, and if having waited for service, leaving the system after being served. Characteristics of a queueing system include:

1. Arrival pattern of customers: Often measured in terms of the average number of customers entering the system per unit time or by the average time between every successive arrival.

2. Service pattern of the servers: service patterns can be as well described as the rate of service or the mean time to accomplish a service.

3. Queueing discipline: Refers to the manner by which customers are selected for service when a queue has formed. The most common disciplines are: first come first served (FCFS), last come first served (LCFS), selection in random which is independent of the arrival order for service (RSS) and a variety of priority schemes.

4. System capacity: The limitation to the amount of waiting room or to the length of the queue that system can hold.

5. Number of system channels: refers to the number of parallel service stations which can serve the customers simultaneously.

6. Number of service stages: The service stations may contain several stages to finish the service.

A queueing system can be denoted by a notation in the form of A/B/X/Y/Z, where A indicates in some way the interarrival distribution, B the ser-

vice pattern as described by the probability distribution, X the number of service channel, Y the restriction of system capacity and Z the queue discipline. In many cases, only the first three symbols are used and we are assuming a queueing system with no capacity constraint and follows a FCFS queue discipline. For example, $M/E_k/1$ stands for a queueing system with exponential arrival, Erlang type k service, one service channel, no limitation to queue capacity and service according to FCFS basis.

5.6.2 Cyclic Queues

Consider a queueing network shown in *Figure 5.7* with the following characteristics:

1. Mean service time for each channel at node i is μ_i

2. Arrival from the "outside" to node i with mean rate r_i

3.The probability that a customer has completed service at node i will go next to node j (routing probability) is r_{ij} (assuming independent of the state of the system), where i = 1, 2,...,k and ri0 indicates the probability that a customer will depart from node i.

A cyclic queue is defined by:

$$r_{ij} = \begin{cases} 1 & (j = i+1; 1 \le i \le k-1) \\ 1 & (i = k, j = 1) \\ 0 & (\text{elsewhere}) \end{cases} \qquad \begin{cases} r_i = 0 & \text{for all i} \\ r_{i0} = 0 & \text{for all i} \end{cases} \qquad (11)$$

which conceptually means that no customer may leave or enter the system and all the customers in the queue are served in a circular manner and when

the last node finishes the service, the customer is then cycled back to the first node

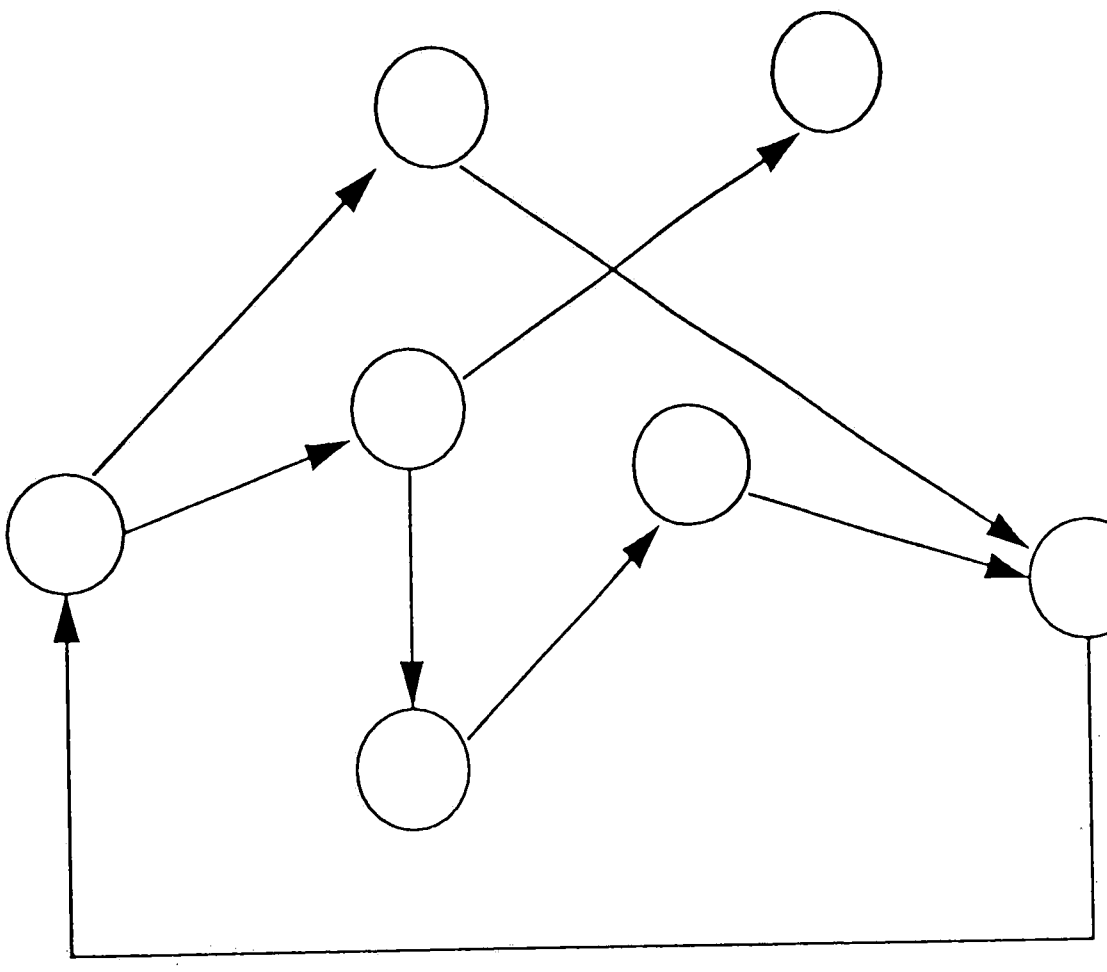

Figure 5.7 A network Model

5.6.3 Queueing Modeling for the Grinding Process

In this thesis it is proposed that a grinding process can be modeled as a queueing system. Consider the events occurring in the cutting zone, each grit on the wheel enters the zone successively, intersects with the workpiece if it is an active grit, generates the chip as a result of the deformation caused by the intersection, and finally leaves the zone. Each active grit can be abstract customer entering an area to be served and the cutting zone is the area where service takes place.

From the four-state Markov chain generated in section 5.5, the probabilistic structure of the incoming active grits is determined and unconditional probability can be calculated which in turn defines the customer arrival distribution. The service area will be defined as the cutting zone depending on the feed rate, depth of cut and wheel speed. According to the factors taken into account to formulate the queueing system, different service disciplines, distributions of the service pattern and the number of channels will be selected. One of the major factors that can be included in this queueing system to enhance the generality of the model, is the abrasive wear which can be classified into two categories, namely, attritious wear and fracture wear. Between the two, the fracture wear is responsible for most of the stochastic behavior of the abrasive wear in the cutting zone. The formation of an appropriate queueing system will depend on how fracture wear is emphasized on.

By assigning more weight for the fracture wear, the service time can take on values from a certain distribution to represent the fracture phenomenon of the abrasives during grinding. From the engineering point of view, the domain of the distribution must be restricted, that is to say, the service time for

an abrasive can not go beyond the time it spends in the cutting zone by a certain wheel speed without breaking. Based on this observation, an appropriate distribution will be the Beta distribution which is:

$$f(x) = \begin{cases} \frac{1}{B(a,b)} x^{a-1}(1-x)^{b-1} & 0<x<1 \\ 0 & \text{otherwise} \end{cases}$$

$$B(a,b) = \int_0^1 x^{a-1}(1-x)^{b-1}dx \qquad (12)$$

In practice, the a and b parameters must be carefully chosen based on the experimental data, The experimental data has to be normalized to be suitable for applying the Beta distribution. If due to the limitation of the available equipment, the a, b parameters can be determined by setting a reasonable value. Based on the above argument, assuming that the grinding proceeds in a steady state, the process can be modeled as a G/G/C queueing system. The number of channels has to be determined by the cutting zone length and the associated profilometer setting.

A different approach for the modeling is by assuming an attritious wear dominated situation. In this case, a finite arrival population is obtained. The entire population is the collection of all the active grits around the wheel circumference. Each grit enters the zone successively and takes away certain amount of the work material as the chip. The service time in this case can also be a Beta distribution with carefully identification of the a, b parameters from the experimental data. Therefore, a cyclic queue is the best to describe

this phenomenon. Again, in order to adjust to the reality, the number of nodes in the cyclic queueing system has to be determined by the numbers of the signals that the cutting zone length can accommodate.

No matter which queueing system is chosen to model the process, steady state probability, the expected number of active grits in the zone can be estimated, the dynamics of the grinding process can also be monitored by simulation.

Chapter 6

Conclusion

Ideas relating to the macro to the micro behavior of the grinding process have been described in this thesis. Creep feed grinding of superalloys by CBN abrasives was first investigated. CBN is a superabrasive that is superior to synthetic diamond in two aspects:

1. Thermal stability up to 1300 °C in normal atmosphere.
2. Chemical stability when grinding steel.

Grinding in creep feed mode has the advantages of high production rate, low thermal damage, less tendency to chatter and high form holding characteristic. Due to this advantage, CBN abrasives combined with creep feed grinding give a very good performance for the machining of the superalloys.

Due to the intricate nature of the grinding process, model building is a complex task. In attempting to control the process, a potential model for monitoring the input/output of the process is strongly in demand.The neural network models were constructed to facilitate the concurrent control and the recognition of an accurate output pattern based on partial system input information. For the two given experimental data sets, the neural networks were able to converge within 20,000 iterations and gave an accurate mapping from the input to the output for the test data sets. The trained neural networks were then fed forward to facilitate the multi-objective optimization. Optimization strategies were visually presented by value-path diagrams and *Table4.1-4.4*.

Surface modeling has been a research area which has received necessary attention from the researchers in material science and geological science. To achieve a precise macro model for the grinding process, the events occurring at the interface of the grits and the workpiece has to be investigated first. To facilitate this, the wheel profile has to be modeled. Different approaches such as time series analysis and stochastic process analysis have been discussed. The author proposes a new approach for the modeling of the wheel profile by fractal analysis which can be extended to three dimensional modeling. The fractal dimensions for vitrified and resinoid wheel profiles were measured by the variation method. Observation was made that coarser the profile the higher the dimension, which means a denser occupation of the metric space by the fractal. Based on the fractal dimension which characterizes the profile, IFS interpolation was carried out to conduct the simulation for each wheel. The resultant simulated profile shows a good approximation of the original profile.

Number of active cutting edges was calculated to give a detailed description in the cutting zone. From the calculation, the finer wheel gave a higher number of cutting edges, which was suitable to achieve the expected result. Four-state Markov chains were then generated which determines the probabilistic structure of the process for each wheel. Based on the matrices, simulations were conducted to generate the distribution of the number of active cutting edges. The Gamma distribution turned out to be an outstanding fit for the data. Based on the statistics and the Gamma parameters, vitrified wheel is superior to resinoid wheel due to less unit load on the active grits.

The last part of the thesis shows the approach to model the micro behavior of the grinding process by treating the active cutting edges as customers and the cutting zone as the service area. Different queueing systems can be applied depending on the wheel wear mechanism. A cyclic queue was demonstrated to be an appropriate model when the process is subjected to more attritious wear than fracture wear. If, instead, fracture wear dominate the wheel wear mechanism, a G/G/C queueing system was proposed to represent an appropriate model for the grinding process.

Based on the research presented in this thesis, the author would like to point out several directions and possible approaches for the future research.

1. Increase the speed of convergence for the learning of the neural network.

2. Escape from the trap of local optimal during the training of the neural network.

Effort has been made during the learning of the neural network to increase the speed of convergency by adjusting the momentum term and the learning rate of the back propagation learning algorithm. The result was successful to some degree although not totally satisfactory. The possible solution to achieve the above objectives is to embed a genetic algorithm as well as a simulated annealing technique in the learning algorithm as pointed out in [49].

3.Three dimensional modeling of the grinding wheel profile.

The final goal for the surface modeling is to provide a three dimensional model for the wheel profile in order to facilitate the "real world" simulation of the process. Possible approaches can be focussed on:

Time Series: To look at the correlation between two time series and based on the model of one time series and the correlation function between the series, construct the entire surface topography.

Stochastic Process Analysis: The approach will proceed as: First, randomly allocate the peaks of the profile according to the distribution function obtained from the experimental data. Second, research the correlation function between peaks. The proposed correlation function is of the form:

$$\rho = \frac{1}{e^{-kx}}$$

where: ρ: correlation between two points on the profile

k: a constant from the experimental data

x: rectangular or euclidean distance between points

Third, construct the surface successively according to the peak location of the correlation function.

Fractal Analysis: It offers a potential in modeling a three dimensional topography. An efficient way of measuring the fractal dimension for a three dimensional object by performing a three dimensional IFS interpolation has to be researched.

4. Software Integration

The author has made an endeavor toward the object-oriented programming for the developed algorithms in this research. An integrated grinding simulation system can be established based on the objects developed so far. More powerful and flexible simulation system can be developed by including the factors like wheel wear, thermal damage and machine tool rigidity.

References

[1] Gardinier, C. F., "Physical Properties of Super Abrasives", Ceramic Bulletin, Vol. 67, No. 6. 1988, pp. 1006-09.

[2] Harry, D. D., and Kumar, D. V., "Technological Fundamentals of CBN Bevel Gear Finish Grinding", SME Conference on Superabrasive, 1985, MR85-273

[3] Malkin, S., "Current Trends in CBN Grinding Technology", Annals of the CIRP, Vol. 34/2, pp.557-563.

[4] Werner, G., and Tawalkloi, T., "Deep Grinding Narrow Slots with CBN Wheels", Industrial Diamond Review, 1988, pp. 285-289.

[5] Werner G., "Increased Removal Rates and Improved Surface Integrity by Creep Feed Grinding", AES Magazine, May-June 1983, pp. 4-10.

[6] Tonshoff, H. K., and Grabner, T., "Cylindrical and Profile Grinding Boron Nitride Wheels", Proceeding of the 5th International Conference on Production Engineering, 1984, pp. 326-344.

[7] Juchem, H. O., "Using Vitrified Bond ABN Wheels", Industrial Diamond Review, June 1986, pp. 243-247.

[8] Kalpakjian S., "Manufacturing Engineering and Technology", Addison Wesley Publishing Company, Reading, Ma., 1989

[9] Andrew C., Howes T.D. and Pearce, "Creep Feed Grinding", Holt, Reinhart and Winston, 1985, New York.

[10] Werner,P.G., "Influence of work material on grinding forces". CIRP Annals, 1978, 27 (1), 243-248.

[11] Kita. Y, Dmalos H. and Salje E. (1980) "Wheel wear in profile grinding". Proceeding 4th International Conference on Production Engineering, Tokyo, 612-19.

[12] Rubsenstein C., "The Mechanics of Grinding", Int. J. Mach. Tool Des. Res., Vol 12,1972, pp. 127-139.

[13] Lortz W., "A Model of Cutting Mechanism in Grinding", Wear, 53, 1979, pp. 115-128.

[14] Rowe G.W.and Wetton A.G., "Theoretical Considerations in the Grinding of Metals", Journal of The Institute of Metals, Vol 97, No 97, 1969, pp. 193-200

[15] Liao, T.W., Sathyanarayanan, G., Storer, R. H., and Wilson, G.R., "Off-line Optimization of Creep Feed Grinding of Alumina Ceramics", in Grinding Fundamentals and Applications, Ed. by S. Malkin and J.A Kovach, ASMF PED vol. 39, 1989,. 241-251.

[16] Shah G.N., Bell A. C.and Malkin S., "Quantitative Characterization of Abrasive Surfaces Using a New Profile Measuring System", Wear, 41 (1977) 315-325.

[17] Dauw ir. D.F., Brown, C. A., Grienthuysen J.P.van and Albert ir.J.F.L.M., "Surface topography investigation by fractal analysis of spark-eroded electrically conductive ceramics", Annals of CIRP Jan. 1990.

[18] Ranganath Nayak P., "Random process model of rough surfaces", Journal of Lubrication Technology, Transaction of the ASME, July 19971, Vol. 92, pp.308-407.

[19] DeVor R.E. and Wu S. M., "Surface profile characterization by autoregressive-moving average models", Journal of Engineering for Industry, Transaction of the ASME, August 1972, Vol 93, pp. 825-832

[20] Boger F., Feder J. and Jossang T. 1987. "Fractal Landscape generated using Voss's successive random addition algorithm", Report Series, Cooperative Phenomena Project, Department of Physics, University of Osolo, 87-15, 1-11.

[21] Falconer K. J., "The Geometry of Fractal Sets", Cambridge University Press, Cambridge, 1985.

[22] Mandelbrot B. B., Passoja D. E. and Paullay A. J., "Fractal character of fracture surfaces of metals", Nature, 1984, 308, 721-722.

[23] Pfeifer P., Avnir D. and Farin D. "Ideally irregular surfaces of dimension greater than two, in theory and practice", Surface Sci., 1983, 126, 569-572.

[24] Wong P.-Z., Howard J. and Lin J.-S., "Surface roughening and the fractal nature of rocks", Schlumberger-Doll Research Preprint, 1985

[25] Jens Feder, "Fractals", Plenumm Press, New York, 1985

[26] Tsuwa H., "An investigation of grinding wheel cutting edges", Journal of Engineering for Industry, Transactions of ASME, November 1964, pp. 371-382.

[27] Law S.S. and Wu S. M., "Simulation study of the grinding process", Journal of Engineering for Industry, Transactions of ASME, November 1973, pp.972-978.

[28] McAdams H.T., "Markov chain models of grinding process", Journal of Engineering for Industry, Transactions of ASME, November 1964, pp.383-388.

[29] Malkin S., "Grinding Technology, Theory and Applications of Machining with Abrasives", 1989, Ellis Horwood Limited.

[30] Stanley, J. and Bak, E., "Introduction to Neural Network", California, 1988.

[31] DARPA, Neural Network Study, Armed Forces Communication and Electronics Association, 1988

[32] Stanley, J., Bak, E., "Introduction to Neural Network", California, 1988.

[33] California Scientific Software, BrainMaker: Neural Network Simulation Software, Users Guide & Reference Manual, California, 1988.

[34] Bayle, A.,"Learning in Neural Networks," PC AI, Nov/Dec, 1988, pp. 40-44.

[35] Bailey, D., Thompson, D., Feinstein, J.,"The Practical Side of Neural Networks: Part One," PC AI, Nov/Dec, 1988, pp. 33-36.

[36] Chryssolouris, G., Guillot M., "A Comparison of Statistical and AI Approaches to the Selection of Process Parameters in Intelligent Machining", Journal of Engineering for Industry, Transactions of the ASME, Vol.122, May 1990, pp. 122-131.

[37] Rangwala, S. and Dornfeld D. A., "Learning and Optimization of Machining Operation Using Computing Ability of Neural Networks", IEEE Trans on System, Man an Cybernetic, Vol. 19, No.2, March/April 1989, pp.299-314

[38] Rangwala, S. and Dornfeld D. A., "Integration of Sensors Via Neural Networks for Detection of Tool Wear States", in Intelligent and Integrated Manufacturing Analysis and Synthesis, ASME PED-25, 1987, pp. 109-120

[39] Rangwala S.and Dornfeld D. A., "Sensor Integration Using Neural Networks for Intelligent Tool Condition Monitoring", ASME, J. of Eng. for Industry, Vol. 112, Aug. 1990, pp. 219-228

[40] Dornfeld D. A."Neural Network Sensor Fusion for Tool Condition Monitoring", Annals of the CIRP, 39/1, 1990, pp. 101-105

[41] Okafor A. C., Marcus M. and Tipirneni R., "Multiple Sensor Integration Via Neural Networks for Estimating Surface Roughness and Bore Tolerance in Circular End Milling", Trans. of NAMRI/SME, 1990, pp. 128-136

[42] Cohen, J.L., "Multiobjective Programming and Planning", Academic Press, New York, 1978

[43] Cupta, O.K. and Ravindran, A., "Branch and Bound Experiments in Convex Nonlinear Integer Programming", Management Science, Vol.31, No.12, dec. 1985, pp.1533-1546.

[44] Barnsley M., "Fractals Everywhere", 1988, Academic Press, Inc. Boston.

[45] Mandelbrot B. B., Possoja D. E., Paullay A. J., "Fractal Characterization of Fracture Surface of Metals", Nature, 1984, 308:721-722.

[46] Jordan D. L., Hollins R. C. and Jakeman E., "Measurement and Characterization of Multiscale Surface", Wear, 19886, 109:127-134

[47] Underwood E.E. and Banjerju K., "Fractals in Fractography", Material Science and Engineering, 1986, Vol.80, pp. 1-14

[48] Dubuc B., Quiniou J.F. Roques-Carmes C., Tricot C. and Zucker S.W., "Evaluating The Fractal Dimension of Profiles", Physical Review, Feb. 1989, Vol. 39, No.3, pp. 1500-1512

[49] Foo Y.P. and Takefuii Y., "Stochastic Neural Networks for Solving Job-Shop Scheduling", IEEE International Conference on Neural Network, 1988, Vol. 2, pp. 275-290

Vita

I-Chung Joseph Lin was born on the sixteenth day of May 1964 in I-Lan Taiwan. He graduated from the Tsing-Hwa university, Taiwan, in July 1986 with a B.S. degree in Industrial Engineering.